SCIENTIA AGROPECUARIA

Scientia Agropecuaria

Web page: http://revistas.unitru.edu.pe/index.php/scientiaagrop

Facultad de Ciencias Agropecuarias

Universidad Nacional de Trujillo

REVIEW

Morphophysiological diversity in rice: A trait-based framework for carbon capture, allocation, and genotype selection

Angélica Alejandra Palma-Araúz[1, 2 *]; Mario Augusto García Dávila[1]; Miguel Antonio Caicedo-Baltodano[3, 4, 5]

[1] Facultad de Ciencias Agropecuarias, Universidad Nacional de Colombia, Palmira Campus, Valle del Cauca, Colombia.
[2] Facultad de Ciencias Agropecuarias, Universidad de Panama, Chiriqui, Panama.
[3] Grupo de Investigación en Diversidad Biológica, Departamento de Ciencias Biológicas, Facultad de Ciencias Agropecuarias, Universidad Nacional de Colombia, Sede Palmira, Valle del Cauca, Colombia.
[4] Fundación para el Estudio de Especies Invasivas (FuEDEI), Hurlingham, Buenos Aires, Argentina.
[5] Consejo Nacional de Investigaciones Científicas y Técnicas (CONICET), Ciudad Autónoma de Buenos Aires, Argentina.

* Corresponding author: apalmaa@unal.edu.co (A. A. Palma-Araúz).

Received: 11 March 2026. Accepted: 20 October 2026. Published: 30 October 2026.

Abstract

Rice (*Oryza sativa* L.) provides a primary source of caloric intake for over half of the global population. Aligning grain production with climate mitigation requires understanding how plant traits influence carbon balance under contrasting water regimes, which affect both trait expression and the fate of plant-derived carbon in soil and greenhouse-gas emissions. Here, the morphological and physiological attributes that govern carbon acquisition, allocation, and retention in rice were reviewed. Belowground, root traits contribute through soil exploration, rhizosphere activity, and structural accumulation, influencing resource acquisition, carbon inputs, and gas transport. Aboveground, shoot architecture, stay-green behavior, and source–sink coordination regulates canopy photosynthesis, reserve remobilization, and allocation to grain and residues. These complementary functions across genotypes, developmental stages, and water regimes, distinguishing plant carbon gain from soil retention and the net greenhouse-gas balance, were examined. Four operational archetypes, deep explorer, source maximizer, sink maximizer, and balanced integrator, are proposed as combinations of candidate traits for rice improvement and management. These proposed selection criteria are distinct from previously published observations, and their combined performance requires field validation. Evaluation would consider calibrated multimodal phenotyping with field measurements of yield, carbon allocation, ecosystem carbon budgets, and greenhouse-gas balances. The central hypothesis proposed as a result of this review is as follows: Combining deep root exploration with a coordinated supply of assimilates, the remobilization of reserves, and grain demand could improve carbon retention while maintaining grain yield, with outcomes that depend on the water regime and the fate of the residues.

Keywords: plant-soil interactions; functional traits; carbon allocation; root architecture; photosynthetic efficiency; source-sink dynamics.

DOI: https://doi.org/10.17268/sci.agropecu.2025.067

Cite this article:

Palma-Araúz, A. A., García Dávila, M. A., & Caicedo-Baltodano, M. A. (2026). Morphophysiological diversity in rice: A trait-based framework for carbon capture, allocation, and genotype selection. *Scientia Agropecuaria, 17*(4), 1027-1047.

1. Introduction

Climate change threatens rice (*O. sativa* L.) productivity through warming, changes in humidity, and atmospheric CO_2 concentration, with responses depending on growing conditions and the timing of exposure (Chauhan et al., 2017; Core Writing Team et al., 2023; Kakar et al., 2021; Kingra et al., 2019; Liu et al., 2023). Droughts and heat waves, together with soil salinization, further jeopardize yield stability across tropical and subtropical regions (Chauhan et al., 2017; Core Writing Team et al., 2023; Ji et al., 2024).

Beyond its climate sensitivity, rice cultivation couples atmospheric carbon uptake with greenhouse-gas emissions (Gangopadhyay et al., 2022; Soremi et al., 2023). Photosynthesis fixes CO_2 into aboveground and belowground biomass, whereas anaerobic decomposition in flooded paddy soils produces CH_4 (Das et al., 2023; Gangopadhyay et al., 2022; Liu et al., 2019; Tang et al., 2019; Win et al., 2020). These soils can also release N_2O through denitrification, so carbon uptake alone does not establish a favorable greenhouse-gas balance (Core Writing Team et al., 2023; Hussain et al., 2015; Ji et al., 2024; Soremi et al., 2023; Win et al., 2020).

Part of the photosynthetically fixed C enters soil through roots and rhizodeposition, where microbial decomposition and stabilization determine its fate (Hussain et al., 2015; Jiménez & Pedersen, 2023; Lu et al., 2003; Pausch & Kuzyakov, 2018; Rizi & Mohammadi, 2023). These pathways connect plant-derived carbon inputs with soil retention and methane transport, both influenced by root traits and management (Aulakh et al., 2000; Das et al., 2023; Tang et al., 2019).

Because plant traits influence both carbon inputs and gas transport, selecting for traits involved in carbon acquisition and allocation can complement agronomic practices to mitigate emissions (Das et al., 2023; Hussain et al., 2015; Jat et al., 2016; Ji et al., 2024; Jiménez & Pedersen, 2023). Recent field studies examine stage-dependent associations between root and shoot traits and CH_4 emissions (Fang et al., 2026), as well as sucrose transport in stem–grain biomass partitioning (Ni et al., 2026). Greenhouse experiments extend this perspective to the rhizosphere, associating altered microbial hydrogen cycling with lower CH_4 emissions in transgenic rice (Shi et al., 2026).

To integrate these lines of evidence, this review examines how coordinated root and shoot responses to aerobic and flooded conditions influence the direction and magnitude of carbon fluxes. Four candidate archetypes translate these relationships into criteria for genotype evaluation across water regimes. Narrative synthesis uses study-specific observations to formulate testable trait combinations, without treating the reported ranges as pooled estimates of subspecies differences or universal agronomic optima.

2. Coordinated functional strategies underlying carbon dynamics in rice

Carbon (C) dynamics in rice agroecosystems connect photosynthetic CO_2 uptake, biomass production and transfer to soil with losses through respiration, methane emissions, and harvest (Haque et al., 2020; Kimura et al., 2004; Liu et al., 2019). Within the soil, organic carbon (SOC) retention reflects the balance between organic inputs and decomposition; stabilization mechanisms and turnover determine how long plant-derived C persists (Dijkstra et al., 2021; Lal, 2004; Trumbore, 2006).

The balance between carbon uptake and losses also depends on soil aeration, as the graphical abstract contrasts nonflooded, more aerated soil with flooded, predominantly anaerobic soil (Kato et al., 2013; Phule et al., 2019). This contrast concerns soil conditions rather than the water source: rainfed lowlands may experience ponding, whereas aerobic treatments may receive irrigation (Y. Kato et al., 2013; Nguyen et al., 2015). Flooding favors methanogenesis, while alternate wetting and drying (AWD) changes soil aeration; drainage may reduce CH_4 emissions but increase CO_2 and N_2O losses (Gangopadhyay et al., 2022; Hussain et al., 2015; Jiménez & Pedersen, 2023; S. Li et al., 2025; Win et al., 2020). Therefore, water management effects require a full greenhouse-gas balance that accounts for residue management.

These water regimes affect plant processes that govern carbon allocation. At the canopy level, leaf area and photosynthetic activity modulate assimilate supply, while grain demand and remobilization of stem reserves influence allocation to harvestable biomass (Yang & Zhang, 2010). The harvest index reflects this aboveground partitioning as grain biomass relative to total aboveground biomass (Fageria, 2007; Haque et al., 2020). Root growth and rhizodeposition transfer assimilates belowground, where microbial processing affects their retention or mineralization (Dijkstra et al., 2021; Liu et al., 2019). Root aerenchyma and barriers to radial O_2 loss regulate gas transport and rhizosphere oxygenation, affecting CH_4 release and oxidation (Jiménez & Pedersen, 2023).

Because carbon inputs and losses occur across different cultivation phases, the temporal basis of accounting matters when integrating these processes. For example, at 3 Mg dry matter/ha of incorporated cover biomass, rice-season net ecosystem carbon balance (NECB) was +1154 kg C ha^{-1}, but annual NECB was −294 kg C/ha (Haque et al., 2020). Table 1 distinguishes carbon balances, soil-stock changes, and belowground allocation on their original measurement bases; Tables S1 and S2 retain the component budgets (Supplementary Material).

Within these accounting boundaries, quantifying C export at harvest requires organ C concentrations and information on grain and straw removal (Haque et al., 2020). Drainage represents another export pathway, with dissolved organic carbon (DOC) losses totaling 9.47–20.30 kg C/ha across three drainage stages in six rice fields in northeastern China (Pu et al., 2021). N_2O contains no C and is therefore excluded from the C mass balance, although its emissions contribute to the greenhouse-gas balance expressed as CO_2 equivalents (Mandal et al., 2021). Carbon budgets quantify aggregate gains and losses but do not resolve the distribution of recently fixed C among plant and soil compartments. Isotopic labeling can examine that distribution, although its estimates depend on the labeling protocol, sampling interval, and compartments analyzed (Liu et al., 2019).

Table 1
Carbon balances, soil-stock changes and belowground allocation in rice studies

Study and temporal basis	Reported quantity and C value	Context and interpretation
Haque et al. (2020) Annual rotation, 2012–2013	NECB (kg C ha^{-1} yr^{-1}): 0 Mg cover biomass: −1,491 3 Mg: −294 6 Mg: −166 12 Mg: +1,247	Barley–vetch followed by flooded rice, South Korea. Cover biomass was incorporated; rice grain and straw were removed. Values describe the entire rotation.
Haque et al. (2020) Crop seasons, 2011–2013	NECB (kg C ha^{-1} $season^{-1}$): Rice: −56 to +2,652 Cover crop: −1,523 to −1,402	Ranges across treatments and two rotations. A positive rice-season balance does not establish a positive annual balance; range endpoints cannot be added.
Mandal et al. (2021) Annual budget, 2018–2019	NECB: +0.63 to +2.51 Mg C ha^{-1} yr^{-1}	Coastal double-rice system, India; contrasting tillage and residue management. The reported budget includes harvest export, gaseous fluxes and runoff C.
Yadav et al. (2019) Annual inputs, 2013–2015	Biomass C inputs: 2.0–3.0 Mg C ha^{-1} yr^{-1}	Rice–rice system, Tripura, India; water regime, tillage and residue treatments. Inputs are not net C retention.
Yadav et al. (2019) Annualized stock change, 2013–2015	Soil C stock increase: 133.6–444.7 kg C ha^{-1} yr^{-1}	Fixed-depth stocks in 0–20 cm soil. Values are tillage means across both water regimes, not separate genotype or irrigation effects.
Z. Zhu et al. (2017) 30 d after pulse labeling	Estimated root + soil C: 2,558; 3,034; 4,583 kg C ha^{-1}	Flooded pots; initial SOC 0.5%, 1.4% and 3.4%, respectively. Isotope-based estimates were scaled by soil mass; they are not annual field-stock gains.

Note. NECB, net ecosystem carbon balance; SOC, soil organic carbon. Cover-biomass rates are Mg dry matter/ha. Original units and accounting boundaries are retained; complete components and protocols appear in Tables S1 and S2 (Supplementary Material).

In pots with three SOC levels, rhizodeposition accounted for approximately 13% – 30% of the labeled C remaining in roots and soil 30 days after a 7-h $^{13}CO_2$ pulse (Zhu et al., 2017). In a separate pot experiment, plants were sampled ten days after $^{13}CO_2$ pulse labeling, and the effects of water regime and fertilization history on C allocation among shoots, roots, and rhizosphere soil differed across tillering, booting, and grain filling (Mi et al., 2026). These short-term tracer observations complement carbon-budget measurements by identifying how newly fixed C is partitioned, but they do not establish the persistence of root-derived inputs in soil.

3. Root system architecture and its role in carbon capture

Root system architecture links soil exploration and resource uptake with root biomass production and the release of organic compounds, thereby influencing carbon inputs and their distribution in rice soils (Freschet et al., 2021a; Freschet et al., 2021b; Hodge et al., 2009; Kuzyakov & Domanski, 2000; Wang et al., 2006).

Once released, root exudates and residues interact with soil biota and mineral surfaces, affecting the retention or mineralization of belowground C inputs (Cheng & Kuzyakov, 2005; Jones et al., 2009a; Kuzyakov & Domanski, 2000; Lu et al., 2003; Poirier et al., 2018). Genotype and water availability modify root development and the distribution of these inputs (Bañoc et al., 2000a, 2000b; Chen & Rengel, 2015; Gu et al., 2017; Guimarães et al., 2020; Kato et al., 2013; Liu et al., 2019; Phule et al., 2019). These effects of root architecture can be examined through three interconnected functions: (1) soil exploration, (2) rhizosphere activity, and (3) structural accumulation (Figure 1) (Brüggemann et al., 2011; Ding et al., 2021; Freschet et al., 2021a; Freschet et al., 2021b; Hodge et al., 2009; Jiménez & Pedersen, 2023; Pierret et al., 2007; Rizi & Mohammadi, 2023). For soil exploration, total root length and vertical distribution influence where C inputs enter soil, whereas tissue chemistry may affect their subsequent decomposition (Figure 1a) (Cheng & Kuzyakov, 2005; Pierret et al., 2007, 2016; Poirier et al., 2018). Their persistence, however, depends on microbial activity and mineral protection as well as on placement (Kuzyakov & Domanski, 2000; Pausch & Kuzyakov, 2018; Poirier et al., 2018). In rainfed lowland field trials in Thailand, fine-root development in the upper layer was lower under non-flooded than flooded conditions; deep-root responses differed between a dry and a wetter year, reflecting soil strength and water availability (Bañoc et al., 2000b; Kato et al., 2013). Field and physiological studies separately link deep rooting with water extraction in rice (Henry et al., 2011, 2012).

Rhizosphere activity influences how these spatially distributed C inputs interact with soil through exudation, microbial associations, and aggregate formation (Figure 1c); fine-root proportion, surface area, and turnover characterize the root-soil interface through which labile C enters soil (Freschet et al., 2021b; Hinsinger et al., 2009; Jones et al., 2009a). Microbial products and aggregates may stabilize part of these inputs (Jones et al., 2009a; Pausch & Kuzyakov, 2018; Poirier et al., 2018), but rhizodeposition can also stimulate decomposition of existing SOC (Cheng & Kuzyakov, 2005; Dijkstra et al., 2021).

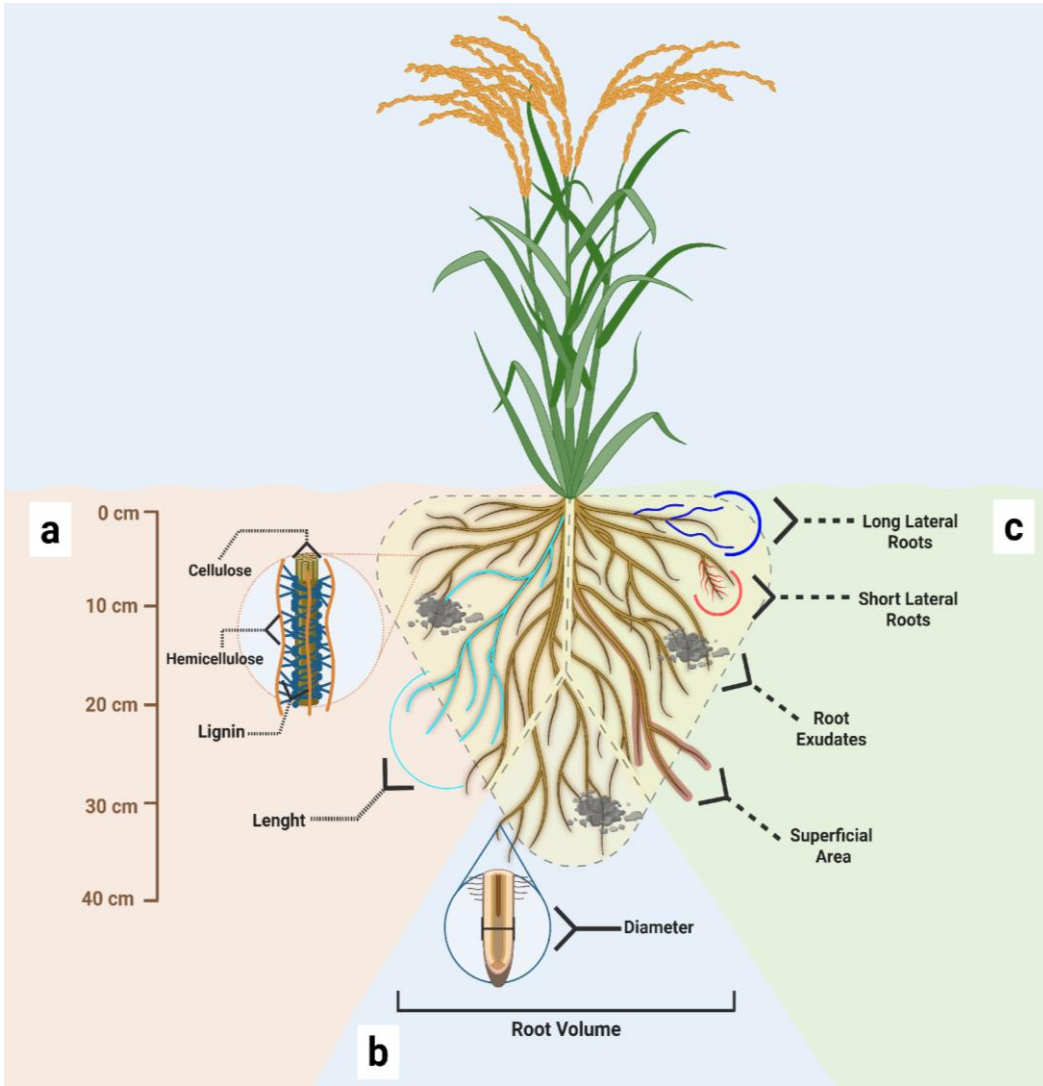


Figure 1. Schematic diagram of rice root system architecture, with key morphological traits grouped into three functional domains: a) soil exploration, b) structural accumulation, and c) rhizosphere activity. (Created with Biorender.com)

Differences in lateral-root development among cultivars change the extent and distribution of this root-soil interface, providing a basis for comparing rhizosphere activity across rice materials and growing conditions (Lafitte et al., 2001; Robin & Saha, 2015; Toyofuku et al., 2015). In flooded pots, Nipponbare and Wuxiangjing 14 had higher fine-lateral-root surface fractions than the *indica* cultivar Yangdao 6, which developed thicker nodal and thick lateral roots (Gu et al., 2017). Interpreting such contrasts requires matching both root classes and denominators. Henry et al. (2011) reported length fractions for fine laterals < 0.05 mm and all laterals < 0.2 mm, whereas Gu et al. (2017) measured surface fractions; the two measures are not interchangeable.

Under saturated conditions, aerenchyma and adventitious roots support internal O_2 transport, while barriers to radial oxygen loss help retain O_2 within roots (Colmer, 2003a, 2003b; Colmer & Pedersen, 2008; Colmer & Voesenek, 2009; Lin et al., 2022). The same gas pathways permit soil-derived CO_2 and CH_4 to move through the plant (Colmer, 2003b; Jiménez & Pedersen, 2023; Kirk et al., 2019). Interpreting these functions requires care with the measurement basis: root porosity in Table 2 measures gas volume, not the anatomical area occupied by aerenchyma. Water regime is equally relevant because genotype and growing conditions affect gas-space development, and its association with CH_4 emissions can reverse between continuous flooding and AWD (Iqbal et al., 2021; Li et al., 2025; Phule et al., 2019).

Beyond exudation and gas transport, structural accumulation (Figure 1b) concerns the quantity and composition of root-derived C entering soil as roots

turn over. Root biomass, nodal-root diameter, and tissue lignin concentration characterize complementary aspects of this contribution (Kuzyakov & Domanski, 2000; Pausch & Kuzyakov, 2018; Poirier et al., 2018; Rasse et al., 2005). Although biomass ratios reported for grasslands illustrate environmental effects, they are not rice thresholds (Hossain & Li, 2021). In rice, water supply and genotype affect root biomass, while tissue chemistry and microbial processing condition subsequent retention (Bañoc et al., 2000a; Liu et al., 2019; Lu et al., 2003; Pump & Conrad, 2014).

Larger root biomass need not supply more persistent inputs. In Park et al.'s (2020) pot and incubation experiments, increased biomass under elevated CO_2 and temperature coincided with lower lignin:N and greater decomposability. The lignin concentrations in Table 2 describe chemical composition, not the proportion of anatomically lignified tissue; neither variable alone establishes long-term SOC persistence (Gul & Whalen, 2013; Poirier et al., 2018). Comparability across scales poses a separate constraint; pot biomass should not be converted into a field selection threshold without a measured ground-area basis.

Individual root traits must therefore be evaluated in combination (Freschet et al., 2021b; Poirier et al., 2018). Axial extension favors access to deeper water, whereas lateral proliferation increases contact with nutrient-rich patches (Bellini et al., 2014; Freschet et al., 2021b; Lynch, 2007). Their balance depends on biomass allocations, development, and soil conditions, which also regulate labile C delivery to the rhizosphere (Cheng & Kuzyakov, 2005; Lu et al., 2003; Pausch & Kuzyakov, 2018; Poirier et al., 2018).

Genetic studies distinguish axial growth from different measures of lateral branching. Horii et al. (2006) reported separate genetic control of root-axis length and a length-based branching index, defined as (total root length − root-axis length)/root-axis length. This index was 18 ± 2 in Akihikari and 31 ± 8 in IRAT 109 in one-month-old upland pot plants (means ± SD). By contrast, the *qLDC5* field comparison in Table 2 counts L-type lateral roots per unit primary-root length at 21 days after sowing (Dinh et al., 2026). The index and count-based density describe different traits, neither of which should be extrapolated directly to branching of mature nodal roots.

These root architectures also depend on nutrient management, as shown by on-farm trials in nutrient-deficient lowlands in Madagascar. Under continuous flooding, the very shallow qsor1-NIL showed a greater yield response to localized P application by P-dipping than IR64 and Dro1-NIL.

Table 2
Root traits: published evidence and proposed screening criteria

Root trait (unit)	Evidence / measurement basis	Screening criterion	Source
Depth (cm) RLD (cm cm^{-3})	Drought, 72 DAS; RLD at 30–45 cm: Dular: 0.24 ± 0.09 IR64: 0.02 ± 0.01	Depth ≥30 cm; greater subsoil RLD or root fraction than the reference.	Henry et al. (2011)
Fine-root surface (%)	Surface fraction varies with root class, cultivar, N and water supply.	Compare equivalent root classes; no fixed cutoff.	Gu et al. (2017)
Root porosity (% gas volume)	Twelve genotypes, 35 d: 20–26% in aerated solution; 29–41% in stagnant, deoxygenated solution.	Assess jointly with radial O_2 loss and CH_4 under each water regime.	Colmer (2003a); Li et al. (2025)
Root biomass (g pot^{-1}; Mg DM ha^{-1})	Dongjinbyeo, loam pots, 114 DAT: 8.3 ± 0.8 versus 16.8 ± 0.4 g pot^{-1}.*	Measure field biomass and C mass by soil depth.	Park et al. (2020)
Root lignin (g kg^{-1} DM); lignin:N	Dongjinbyeo:* lignin: 151 ± 1; 138 ± 3 lignin:N: 54 ± 1; 36 ± 1	Measure chemical composition, not anatomical tissue percentage.	Park et al. (2020)
Lateral-root density (number cm^{-1} of axis)	Madagascar field; L-type, primary roots, 21 DAS: 0.9–1.8 (NERICA4 allele); 3.0–4.7 (DJ123 allele).	Match axis, root class and age; evaluate jointly with depth.	Dinh et al. (2026)
Nodal-root diameter (mm)	Yangdao 6: 0.662–0.743; Nipponbare/Wuxiangjing 14: 0.486–0.556 (pots).	Assess penetration, construction cost and porosity together.	Gu et al. (2017); Fonta et al. (2022)
Root turnover ($time^{-1}$)	Repeated root observations; not tracer loss.	Define estimator, interval and root class; retain continuous values.	Freschet et al. (2021a)

Note. The depth cutoff is proposed, not validated; other traits remain continuous. *Ambient versus elevated CO_2 and temperature. RLD, root length density; DM, dry matter; DAS/DAT, days after sowing/transplanting. Uncertainties are SE; ranges are study-specific.

By comparison, the deeper-rooting Dro1-NIL showed the strongest response to N top-dressing after P-dipping (Oo et al., 2025). Under drought, greenhouse mesocosm and field rainout shelter experiments identified alternative trait combinations: greater nodal-root number and depth occurred with either smaller nodal roots or larger roots with more aerenchyma (Fonta et al., 2022). Performance was assessed through shoot biomass and interpreted in terms of reduced metabolic costs per unit root length (Fonta et al., 2022).

Table 2 pairs study-specific root measurements with exploratory screening criteria. Root turnover must be estimated from root production or mortality relative to standing biomass and a defined interval; neither exudation nor tracer loss measures replacement directly (Freschet et al., 2021a; Pausch & Kuzyakov, 2018). Although root architecture affects the depth of soil C inputs, its contribution to grain production also depends on whether water and nutrient acquisition can sustain the shoot processes examined next.

4. Source-sink coordination and aerial architecture as determinants of carbon capture efficiency

The allocation of assimilated carbon to grain depends on the coordination of photosynthetic supply, stored reserves, and sink demand (Fageria, 2007; Shi et al., 2013; Stella et al., 2016; Ueda et al., 2025; Vishwakarma et al., 2024). Water availability modifies this coordination through its effects on photosynthesis and reserve remobilization, linking shoot function to the root responses described in Section 3 (Yang & Zhang, 2010).

During grain filling, developing grains receive assimilates from photosynthesis after heading, including that of the flag leaf, and from non-structural carbohydrate (NSC) reserves accumulated beforehand as starch and soluble sugars in culms and leaf sheaths (Bueno & Lafarge, 2009; Mohapatra & Sahu, 2021; Tanaka et al., 2022). Remobilization of these reserves helps sustain grain filling when photosynthetic supply is constrained (Stella et al., 2016; Ueda et al., 2025; Vishwakarma et al., 2024; Yang & Zhang, 2010). Earlier estimates cited by Zhang et al. (2017) placed the contribution of culm reserves at 20% – 40% of grain carbohydrate accumulation.

The photosynthetic contribution during grain filling is partly shaped by canopy architecture, which determines how light is intercepted and distributed among leaves (Burgess et al., 2017; Tanaka et al., 2022; Vishwakarma et al., 2024). In glasshouse microplots of five rice genotypes sampled at 45 and 85 days after transplanting, 3D reconstruction and ray tracing associated more upright leaves with deeper light penetration, whereas leaf-area index (LAI) showed no clear relationship with modeled carbon gain per unit ground area (Burgess et al., 2017).

Alongside canopy architecture, delayed leaf senescence can prolong photosynthetic activity during grain filling. Its effect on grain production depends on whether assimilate supply coincides with developing sink demand (Mohapatra et al., 2011; Stella et al., 2016; Ueda et al., 2025).

This dependence on grain demand reflects the distinction between sink size, determined by grain number and potential size, and sink strength, the physiological capacity of developing grains to import and store carbohydrates (Figure 2; Paul et al., 2017; Tu et al., 2022). When transport and assimilate supply are sufficient, sink activity can alleviate feedback inhibition of photosynthesis (Paul et al., 2017; Ueda et al., 2025).

These source–sink interactions influence aboveground biomass partitioning, commonly assessed at maturity through the harvest index (HI), defined as the ratio of grain dry mass to total aboveground dry mass (Fageria, 2007; Yang & Zhang, 2010, 2023). Although increasing HI is an established breeding objective (Shi et al., 2013; Yang & Zhang, 2010, 2023), a higher value does not necessarily indicate greater grain yield or additional carbon capture. Its complementary fraction, 1−HI, represents non-grain aboveground biomass but excludes roots and does not quantify carbon returned to or retained in soil (Fageria, 2007; Yang & Zhang, 2010).

Post-anthesis soil drying shows why biomass partitioning and grain production must be assessed separately. In field experiments averaged over 2005–2007, severe drying increased HI but reduced grain yield in Zhendao 88 and Liangyoupeijiu relative to well-watered plants, whereas moderate drying maintained yield in Zhendao 88 and increased it in Liangyoupeijiu (Yang & Zhang, 2010). Figure 2 illustrates the underlying source–sink relationships through coordinated supply and demand and their respective limitations; it does not represent a measured carbon balance.

The canopy traits in Table 3 address aspects of source function not captured by HI. LAI expresses leaf area per unit ground area, while specific leaf area (SLA) relates leaf area to leaf dry mass. Their interpretation across *indica*, *japonica*, hybrids and introgression lines require attention to genetic background and measurement conditions (Lu et al.,

2009; Mao et al., 2010; Vaughan et al., 2008). Because these traits were measured under different protocols, apparent genetic contrasts require qualification. In a panel of 203 *O. sativa* accessions, HI varied with genotype and genotype × location, and its air-dried mass basis limits comparison with oven-dry measurements (Li et al., 2012). LAI observations from *japonica* cultivars and intersubspecific hybrids came from separate studies; planting density also differed between rice types in the hybrid comparison (Liu et al., 2022; Xu et al., 2020). For SLA, calculations based on genotype-mean leaf mass per area (LMA) and unequal nitrogen supply in a heading-stage comparison limit direct interpretation of cultivar differences (Fukuda et al., 2025; Xiong et al., 2016; Ye et al., 2020).

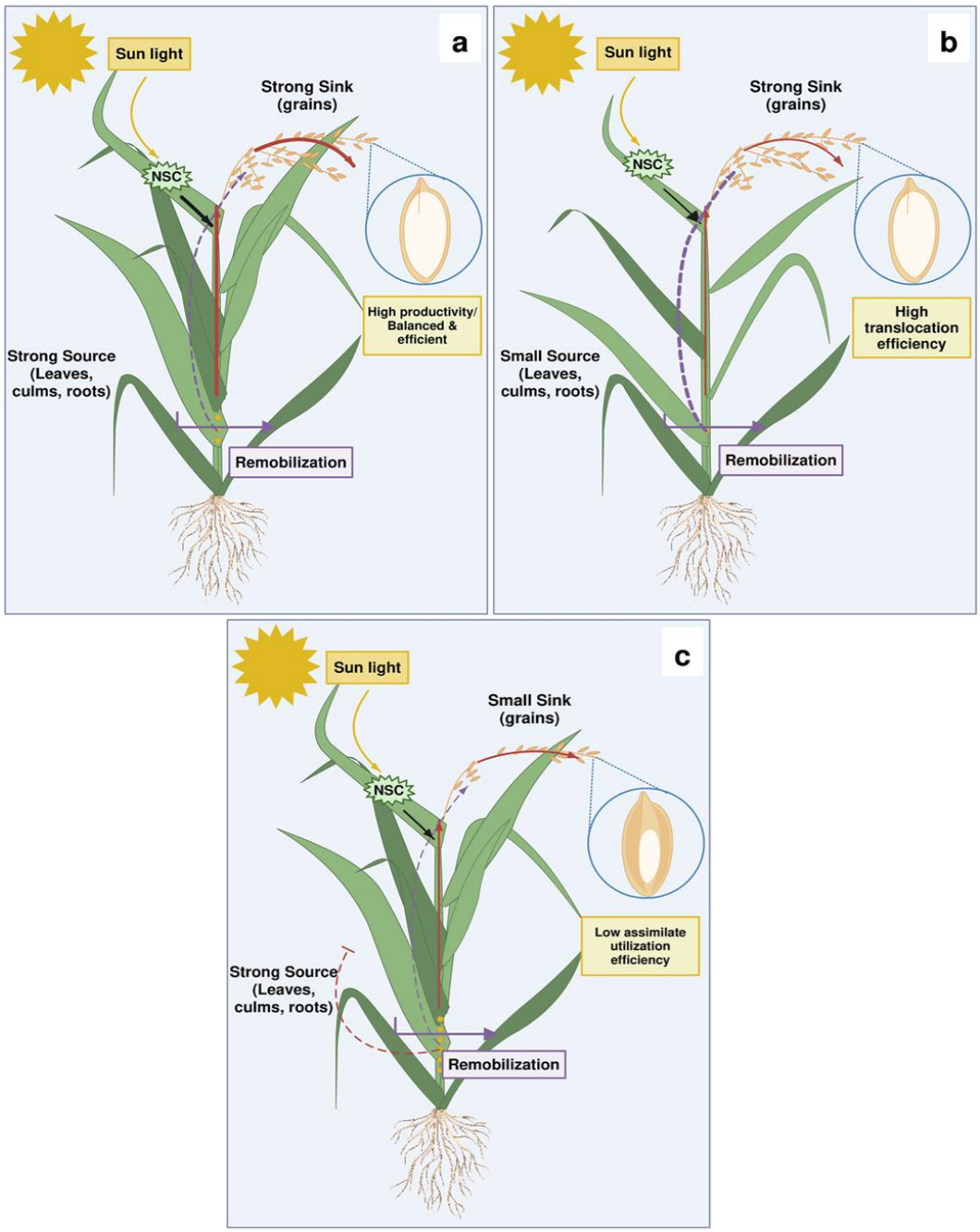


Figure 2. Source–sink scenarios and grain filling in rice: (a) Current assimilation and reserve export meet grain demand. (b) Limited current assimilates supply increases reliance on reserves; this need does not result from smaller leaf area alone. (c) A smaller or less effective grain sink retains more assimilation in vegetative tissues and may feedback on photosynthesis. Gold arrows represent incident light; black/red arrows represent assimilate transport; purple arrows represent reserve remobilization and export. Gold stem circles indicate NSC reserves, and the dashed red line with a bar denotes potential feedback inhibition. Endosperm insets are schematic, not quantitative measures of filling. Adapted from artwork created with BioRender.com.

Table 3
Genotypic variation in HI, LAI, and SLA under defined growth and measurement conditions

Trait and unit	Materials represented	Study-specific values	Environment, measurement and source
HI (fraction)	203 *O. sativa* accessions; *indica*, temperate/tropical *japonica*, aus, aromatic and admixed backgrounds	Stuttgart: 0.0340–0.4506 Beaumont: 0.0625–0.6002	USA, 2009; flooded field plots, 55 kg N ha^{-1}; three blocks. Mature, air-dried plant and grain masses. Whole-panel ranges, not subgroup ranges (Li et al., 2012, Table 1).
HI (kg kg^{-1})	Zhendao 88 (*japonica*); Liangyoupeijiu (*indica* hybrid)	Zhendao 88: 0.46–0.52 Liangyoupeijiu: 0.44–0.50	Yangzhou, 2005–2007 means; 150 kg N ha^{-1}. Standing water or −25/−50 kPa from nine days after anthesis to maturity (Yang & Zhang, 2010).
HI (kg kg^{-1})	CSSL #19 and #91; Yangdao 6 *indica* background	#19: 0.3132–0.4908 #91: 0.4330–0.5682	Yangzhou, 2023–2024; 0, 120 and 240 kg N ha^{-1}. Published percentages converted to fractions (Ni et al., 2026).
LAI (m^2 m^{-2})	Six semi-waxy *japonica* cultivars	6.69–8.32	Total LAI at heading; Taizhou, 2018–2019; 270 kg N ha^{-1}; three blocks. Range across cultivar-year means (Liu et al., 2022, Table 4).
LAI (m^2 m^{-2})	Six *japonica/indica* hybrids; two conventional *japonica* cultivars	Hybrids: 7.38–7.68 Conventional *japonica*: 6.75–6.84	Heading; Ningbo, 2017–2018; 270 kg N ha^{-1}; three blocks. Spacing and seedlings per hill differed between rice types (Xu et al., 2020, Table 3).
LAI (m^2 m^{-2})	Zhendao 88; Liangyoupeijiu	Zhendao 88: 5.1–8.4 Liangyoupeijiu: 4.8–7.8	Full heading; Yangzhou, 2006–2008 means; 150 kg N ha^{-1}. Flooding or reirrigation at −15/−30 kPa from 10 d after transplanting (Yang & Zhang, 2010).
LAI (m^2 m^{-2})	Jing 565 and Nanjing 9108 (*japonica* in the source)	Jing 565: 6.23–6.77 Nanjing 9108: 6.32–7.43	Heading: Hubei, 2017–2018; 270 kg N ha^{-1}; contrasting natural temperature regimes. Jing 565 spans scenarios A/B (Tu et al., 2022, Table 3).
SLA* (m^2 kg^{-1})	Eight *O. sativa* genotypes; panel not stratified by genetic group	13.9–22.2	Newly expanded flag leaves; Wuhan, 2015; flooded outdoor pots, 2 g N pot^{-1}. Calculated from genotype-mean LMA, 45.0–71.7 g m^{-2} (Ye et al., 2020, Table 1).
SLA* (m^2 kg^{-1})	Six *O. sativa* cultivars at sufficient N; four at low N. Five wild entries excluded	Sufficient N: 22.8–27.7 Low N: 19.5–28.7	Young fully expanded leaves, from 40 d after transplanting; Wuhan, 2013; flooded outdoor pots. N: 3.0 or 0.5 g pot^{-1} (Xiong et al., 2016, Tables 1–2).
SLA* (m^2 kg^{-1})	Hokuriku 193 (*indica* type); Nipponbare (temperate *japonica*)	Hokuriku 193: 24.5–32.5 Nipponbare: 24.3–29.4	Nagoya, 2019; 44, 66 and 91 d after transplanting; heading values 28.5 and 24.6. N rates were 190 and 90 kg ha^{-1}, respectively, at 15 × 30 cm spacing with three seedlings per hill (Fukuda et al., 2025).
SLA* (m^2 kg^{-1})	Jing 565; Nanjing 9108	Jing 565: 15.5–19.9 Nanjing 9108: 15.9–19.9	Heading leaves; same field contrasts as their LAI row. Calculated as 100/SLW, with SLW in mg cm^{-2} (Tu et al., 2022, Table 3).

Note. HI, harvest index; LAI, leaf area index; SLA, specific leaf area; LMA, leaf mass per area; SLW, specific leaf weight; CSSL, chromosome single-segment substitution line. Ranges are study-specific, not subspecies reference intervals; HI comparisons also require compatible drying protocols. *With LMA expressed in g m^{-2}, SLA (m^2 kg^{-1}) = 1000/LMA. Values calculated from genotype-mean LMA/SLW are reciprocals of the means, not averages of individual-leaf SLA. Additional source values, material lists, and calculations are provided in Tables S3–S6 (Supplementary Material).

Assimilate movement toward developing grains also depends partly on stem vascular architecture (Fei et al., 2019; Li et al., 2022; Liao et al., 2021). In a panel of 529 accessions, *indica* had more large vascular bundles and greater total bundle area, whereas *japonica* had larger individual bundles (Liao et al., 2021). In *indica* × *japonica* recombinant inbred lines examined at three locations, *indica* ancestry was associated with the number of large vascular bundles, and *DEP1*-associated variation was linked to ABA signaling through AP2-like genes (Fei et al., 2019). In a separate pot study of eight conventional and hybrid cultivars, basal-internode vascular traits were associated with apparent NSC translocation and grain yield (Li et al., 2022).

Beyond vascular capacity, sucrose delivery to the grain depends on regulated loading, transport, and unloading. At the source, flag-leaf transcriptomics revealed genotypic variation in sucrose-metabolism gene expression, although transcript abundance does not quantify carbon flux (Nguyen et al., 2015). At the sink, sucrose can be unloaded through symplastic connections or apoplastic routes involving SUT/SWEET transporters and cell-wall invertase (Li et al., 2026; Mohapatra & Sahu, 2021). Among these transporters, OsSUT1 mediates proton-coupled

sucrose uptake (Mohapatra & Sahu, 2021). In Liangyoupeijiu and Shanyou 63, superior spikelets generally showed higher expression of OsSUT1, OsSWEET4, OsSWEET11, and OsSWEET14; higher cell-wall invertase activity; larger phloem areas; and greater plasmodesmal density than inferior spikelets at seven days after anthesis (Li et al., 2026). The expression of these transport-related genes also varies by genotype and grain-filling stage. In Yangdao 6-background *indica* chromosome single-segment substitution lines, #91 had higher HI and apparent stem NSC remobilization than #19, associated with greater stem expression of *OsSUT1*, *OsSUT2* and *OsSWEET13* and grain expression of *OsSUT2*, *OsSWEET11* and *OsCIN1* at seven days after heading under 0, 120 and 240 kg N/ha (Ni et al., 2026). In Yongyou 12 and Yongyou 9, *OsSUT1* expression was similar at 15 days after flowering but higher in Yongyou 12 at 30–40 days (Chen et al., 2022). Genetic variation in this pathway is also evident from the *OsSUT1* allele SUT1-2, present in 74.0% of 123 *indica* cultivars and 6.3% of 192 *japonica* cultivars; these frequencies do not establish differences in transport capacity (Kato & Horibata, 2011).

Hormones also link water status to reserve use and grain development. During post-anthesis drying, higher abscisic acid (ABA) concentrations in leaves and stems were associated with greater remobilization, and exogenous ABA enhanced this response; declining leaf cytokinins accompanied senescence (Yang & Zhang, 2010). Under moderate AWD, recovery of root zeatin and zeatin riboside after rewatering was associated with improved leaf photosynthesis. Cytokinins also support early endosperm cell division (Mohapatra et al., 2011; Yang & Zhang, 2010).

Once carbohydrates reach the grain, starch deposition involves invertases, sucrose synthase, ADP-glucose pyrophosphorylase, starch synthase, and starch-branching enzyme. Zang et al. (2024) associated irrigation-related changes in their activities with better filling of inferior spikelets. These processes govern the use of imported assimilates, whereas the rate of CO_2 acquisition must be assessed independently through the physiological measurements considered next.

5. Physiological determinants of carbon assimilation and retention

The source–sink relationships described above help explain carbon allocation within rice plants but do not, by themselves, demonstrate its retention in soil. Carbon gain and allocation in C_3 rice also depend on processes governing CO_2 uptake, photochemical energy conversion, and plant water status (Ferguson et al., 2020; Guo & Lv, 2025; Kalaji et al., 2017; Wu et al., 2014). These processes can be considered within three interconnected functional components: (1) gas exchange and water-status regulation, (2) photochemical efficiency and energy dissipation, and (3) redistribution and utilization of fixed carbon across developmental stages (Figure 3; Ohsumi et al., 2008; Oue, 2023; Zhu et al., 2010).

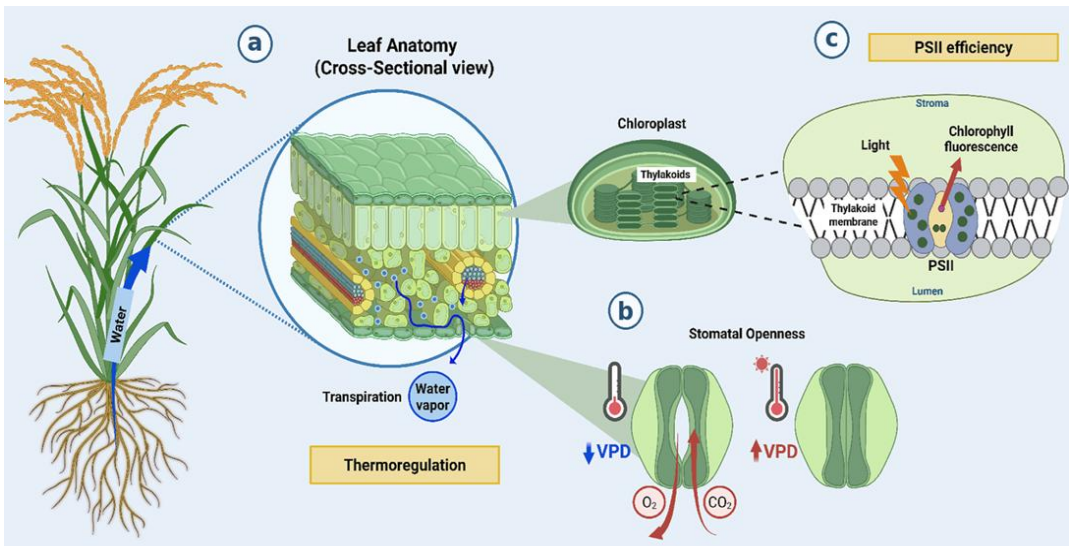


Figure 3. Physiological processes involved in carbon capture in rice. The labeled domains depict (a) rice leaf anatomy and the pathway for CO_2 diffusion and transpiration; (b) stomatal regulation of CO_2 and water-vapor exchange under contrasting vapor-pressure deficits; and (c) chloroplast photochemistry involving PSII and chlorophyll fluorescence. These are conceptual processes, not quantitative measurements of carbon flux (Created with Biorender.com).

Table 4
Reported physiological values, measurement conditions, and functional trade-offs in rice

Variable (unit)	Observed / fitted values	Measurement setting	Sources
Stomatal conductance, g_s (mol H_2O m^{-2} s^{-1})	Heading–flowering: 0.280–0.363 Thereafter: 0.255–0.327	Koshihikari, Himenorin, Nikomaru; ponded screen-house boxes. Flag leaves, LI-600PF, 08:30–12:00 JST; comparable ambient light.	Oue (2023)
Effective PSII yield, ΦPSII (dimensionless)	Control: 0.39 ± 0.02 Alkaline: 0.27 ± 0.02	ChangBai-9 seedlings; 30 d at 35 mM carbonate/bicarbonate, pH 8.9. LI-6400x; actinic-light and pulse settings NR.	Wu et al. (2014)
Leaf–air temperature, ΔT (°C)	−2.55 to −0.73 (four group means)	22 varieties/lines; upland field, Mito. Top unfolded leaves, 13:00–15:00; infrared leaf and concurrent air temperatures.	Hirayama et al. (2006)
Transpiration, E (mmol H_2O m^{-2} s^{-1})	Control: 4.71 ± 0.14 Alkaline: 3.48 ± 0.14	ChangBai-9; same alkaline treatment. Expanded blades, 08:30–10:30, LI-6400x; PPFD 1200 µmol photons m^{-2} s^{-1}.	Wu et al. (2014)
Leaf temperature (°C; modeled)	Assimilation peak: 30.8 Strongest g_s acceleration: 34.2	Huanghua Zhan, climate chambers. Youngest expanded/flag leaves, 09:00–12:00; VPD-based model pooled treatments, stages and years.	Zhao et al. (2026)
Apparent ETR (µmol electrons m^{-2} s^{-1})	Heading–flowering: 136.0–169.6 Thereafter: 138.6–166.9	Same flag-leaf protocol as g_s; ambient light. Flash 7000 µmol photons m^{-2} s^{-1}; absorptance 0.85, PSII allocation 0.5 assumed.	Oue (2023)
Maximum PSII yield, F_v/F_m (dimensionless)	Control: 0.82 ± 0 Alkaline: 0.77 ± 0.01	ChangBai-9; same treatment. LI-6400x; dark-adaptation duration and saturating-pulse settings NR.	Wu et al. (2014)

Note. Ranges span cultivar/group means; Wu et al. values are means ± SE (n = 5; zero SE as reported). ΔT = leaf minus air temperature. PPFD, photosynthetic photon flux density; VPD, vapor pressure deficit; ETR, electron transport rate; NR, not reported. Growth conditions and additional settings: Table S7 (Supplementary Material). Values are not universal optima.

Stomatal conductance (g_s) regulates CO_2 entry into the leaf while coupling assimilation to transpirational water loss (Lawson & Blatt, 2014; Ohsumi et al., 2008; Oue, 2023; Xiong, 2024). Rising vapor pressure deficit (VPD) and declining soil moisture can therefore restrict g_s and CO_2 assimilation, while boundary-layer and mesophyll diffusion impose additional constraints on CO_2 supply to chloroplasts (Lawson & Blatt, 2014; Ohsumi et al., 2008; Ouyang et al., 2017). Variation in net photosynthesis is also evident across cultivars: in a greenhouse comparison under aerobic cultivation at 50% flowering, CR Dhan 202 showed higher net photosynthesis than BPT 5204 (Phule et al., 2019).

Because transpiration influences leaf temperature, leaf–air temperature differences can provide additional information on the coupling between water loss and CO_2 uptake under upland conditions, although their interpretation remains context-dependent (Hirayama et al., 2006). The photosynthetic response to temperature also varies with developmental stage and nitrogen supply (Ye et al., 2022). Illustrating the complexity of these responses, a VPD-based model fitted to gas exchange across treatments, stages, and years in Huanghua Zhan rice grown in climate chambers showed declining assimilation at high leaf temperatures despite increasing g_s and transpiration (Zhao et al., 2026).

Gas-exchange measurements characterize net CO_2 exchange but do not directly describe the photochemical processes supporting assimilation. Chlorophyll fluorescence provides complementary information through indicators such as effective PSII quantum yield (ΦPSII), which reflects photochemical efficiency under light, and dark-adapted Fv/Fm, which estimates maximum PSII efficiency (Kalaji et al., 2017). Their responses vary with irradiance, spectral quality, cultivar, and heat stress (Ferguson et al., 2020; Quero et al., 2019). Apparent electron transport rate (ETR) additionally depends on irradiance and assumptions about leaf absorptance and excitation allocation to PSII. Because electron transport supports photorespiration and other sinks besides CO_2 fixation, neither ETR nor ΦPSII directly measures carbon assimilation (Kalaji et al., 2017; Oue, 2023).

The interpretation of these physiological indicators also depends on developmental stage and stress exposure, particularly during reproduction, when leaf senescence and stress tolerance can modify photosynthetic function (Falqueto et al., 2010; Moradi & Ismail, 2007; Oue, 2023). In BRS Firmeza and BRS Pelota, flag-leaf chlorophyll content and PSII activity followed different senescence trajectories, yet the stay-green cultivar BRS Firmeza had lower grain yield in that comparison (Falqueto et al., 2010). Moradi & Ismail (2007) also observed genotypic differences under stress in the salt-tolerant lines IR651 and IR632, which maintained photosynthetic function better than the sensitive cultivar IR29 under the seedling- and reproductive-stage salinity treatments examined. Consequently, sustained leaf

function should be interpreted together with grain yield rather than treated as its proxy.

This dependence on experimental context is reflected in Table 4, which presents observed physiological values alongside plant material, developmental stage, treatment, and measurement setting rather than as universal optima. Meaningful comparisons require documenting irradiance, temperature, CO_2 concentration, and evaporative demand (Kalaji et al., 2017; Lin et al., 2026; Oue, 2023). For example, Lin et al. (2026) measured leaves at booting–flowering between 08:00 and 13:00, using 400 µmol CO_2 mol^{-1}, a photosynthetic photon flux density (PPFD) of 1500 µmol photons m^{-2} s^{-1}, 30°C leaf temperature, and a leaf-to-air VPD of 1.5 – 2.5 kPa. Because plant growth conditions and instrument settings describe distinct aspects of the experimental environment, additional protocol details are recorded separately in Table S7 (Supplementary Material).

6. Relevance of functional phenotyping for carbon-oriented genotype selection

High-throughput phenotyping (HTP) offers aerial and proximal measurements of canopy development as well as 3D imaging of shoot and root architecture (Chawade et al., 2019; Li et al., 2014; Pieruschka & Schurr, 2019; Reynolds et al., 2020; Watt et al., 2020). To inform carbon-oriented selection, these signals must be calibrated against measured traits at matching spatial and developmental scales (Paez-Garcia et al., 2015; Takahashi & Pradal, 2021). Table 5 summarizes these signals, their applications, and principal limitations.

In combination, vegetation indices and thermal imagery inform canopy growth and water status, while 3D reconstruction and root imaging describe architectural traits that can be evaluated alongside grain filling (Chen & Rengel, 2015; Jones et al., 2009b; Li et al., 2014; Maqbool et al., 2022; Sharma et al., 2024; Tang et al., 2024). These measurements are not interchangeable: canopy background, developmental stage, and atmospheric conditions affect their relationships with biomass and water status, while geometric reconstructions do not directly measure carbon allocation (Chawade et al., 2019; Kaya, 2025; Luan et al., 2021; Mayanja et al., 2024; Mertens et al., 2023).

These limitations are particularly restrictive belowground. X-ray computed tomography (CT) provides detailed root images, but root–soil contrast, substrate water content, processing time, and the trade-off between sample volume and resolution limit its application to field-grown plants (Hou et al., 2022; Li et al., 2022). Zheng et al. (2026) improved maize root segmentation using calcined clay–loam mixtures for axial roots and floral foam for fine roots; however, their mature-root workflow still required physical sectioning, separate scans, and digital reassembly. The applicability of this approach to mature rice in flooded field soil remains unestablished (Zheng et al., 2026).

A different scale-related constraint applies to sun-induced chlorophyll fluorescence (SIF), which provides information on photosynthetic activity from field canopies to satellite observations. However, its retrieval depends on high spectral resolution, signal-to-noise ratio, and atmospheric, illumination, and viewing conditions (Deng et al., 2025; Mohammed et al., 2019; Yang et al., 2018). Canopy structure and absorbed radiation further complicate interpretation, and satellite footprints may exceed individual breeding plots (Fu et al., 2022; Mohammed et al., 2019). In a rice free-air CO_2 enrichment (FACE) experiment at Danyang in 2023–2024, canopy SIF reflected leaf photosynthetic responses to elevated CO_2 in Wuyunjing 23, although gross primary productivity (GPP) was not directly measured because the plots were too small for flux-based monitoring (Ye et al., 2026).

Measurement performance must therefore be considered alongside the throughput and cost of deploying each sensor combination at breeding scale. Because economic feasibility depends on equipment costs, the complete workflow, and infrastructure use, shared facilities, standardized protocols, and adequate utilization can improve access (Reynolds et al., 2019, 2020; Rosenqvist et al., 2019). Operational requirements nevertheless differ across uncrewed aerial vehicles (UAVs), portable thermal sensors, terrestrial LiDAR, and laboratory CT (Kaya, 2025; Li et al., 2022; Li et al., 2014).

Published cost estimates show why budgets must specify the measurement unit and services included. For a high-demand UAV scenario, Reynolds et al. (2019) estimated USD 91,000 for 1,700 microplots over ten observation days, equivalent to approximately USD 53.5 per microplot per experiment. The budget included plot management, image acquisition and analysis, trait analysis, and ten-year data storage, assuming existing analysis pipelines and labor conditions in France, the UK, USA, and Germany. These historical, scenario-specific estimates are not current quotations or costs for a complete carbon and greenhouse-gas budget.

Table 5
Phenotyping signals, applications and principal limitations

Technology	Measured signal	Application and main limitation	Sources
Multispectral imaging	Reflectance	Canopy cover/biomass estimates; calibration, background and saturation effects.	Chawade et al. (2019); Fu et al. (2022)
Infrared thermography	Surface temperature	Water-status assessment; sensitivity to wind, radiation and mixed pixels.	Jones et al. (2009b); Wen et al. (2023)
LiDAR	3D canopy geometry	Architecture/biomass estimates; rice-specific calibration and occlusion.	Chawade et al. (2019); Tang et al. (2024)
X-ray CT	3D roots in scanned volume	Rice seedlings in foam; mature-root validation in flooded soil pending.	Li et al. (2022); Zheng et al. (2026)
SIF	Chlorophyll fluorescence	Rice FACE photosynthetic response; structural/radiative effects; GPP not measured.	Mohammed et al. (2019); Ye et al. (2026)

Note. CT, computed tomography; LiDAR, light detection and ranging; SIF, sun-induced chlorophyll fluorescence; FACE, free-air CO_2 enrichment; GPP, gross primary productivity. Each signal requires trait-specific calibration; validity in one crop or substrate does not extend to rice environments.

Rice-breeding consultations in India provide a different cost context, estimating USD 5 per F_6 line in a 5-m phenotyping row and USD 20 per F_6 line in a 10-m^2 yield-trial plot at one location (Anilkumar & Bernardo, 2026). These per-line and per-plot figures describe different services and cannot be converted into a comparable per-hectare carbon-assessment cost; neither includes the complete carbon and gas-flux measurements proposed here. Cost considerations must therefore be accompanied by assessments of technology readiness for each application and environment rather than reliance on a platform-level score (U.S. Department of Agriculture, 2018).

After sensor choice and budgeting, multimodal analysis requires aerial, proximal, and belowground observations to be synchronized and spatially linked to plot identity and developmental stage before machine-learning models can integrate them (Furbank & Tester, 2011; Kaya, 2025; Li et al., 2014). At the canopy scale, DFM-Net illustrates this integration by combining separate RGB and thermal-infrared branches with handcrafted color, texture, and temperature features and using adaptive weights to estimate SPAD, a proxy for chlorophyll status in rice (Tang et al., 2026).

DFM-Net was trained on the 2024 Baiyun dataset and tested externally on 76 plot-stage observations from 38 cultivars at Zengcheng in 2025. Its predictive performance varied by developmental stage, with external-test R^2 values of 0.95 at tillering and 0.79 at heading, and root mean squared errors of 2.76 and 4.18 SPAD units, respectively. Because full radiometric calibration was unavailable, reflectance- and temperature-related features were treated as normalized quantities (Tang et al., 2026). The reported accuracy must nevertheless be interpreted in light of external testing restricted by rainfall to two growth stages and model selection without an independent validation subset. The datasets also differed in sites, years, cultivars, and plot sizes (Tang et al., 2026). Assessing transferability therefore requires keeping repeated observations from the same experimental unit within a single data partition, together with genotype-disjoint and independent season or location tests (Reynolds et al., 2020; Tang et al., 2026). Furthermore, accurate SPAD predictions cannot establish carbon assimilation without independent gas-exchange validation (Fu et al., 2022; Tang et al., 2026).

These calibrated measurements can support genotype selection only when organized around explicit biological hypotheses. We therefore propose four functional archetypes for O. sativa to be examined across indica, japonica, hybrids, and introgression lines (Figure 4 and Table 6). Each emphasizes a different combination of root acquisition, assimilate supply, and grain utilization, without assuming that favorable trait values establish carbon retention (Fageria, 2007; Liu et al., 2019; Watt et al., 2020). Candidates should be compared with a prespecified reference cultivar within the same water regime and under matched nutrient supply, planting density, and developmental stage. Continuous trait values are retained where the profiles overlap.

Deep-explorer. This profile emphasizes subsoil resource acquisition, evaluated through the proposed depth target and greater root length density or root fraction below the main surface layer (Tables 2 and 6). Root biomass and lignin concentration then describe the quantity and chemistry of the inputs placed at depth. This provisional depth screen reflects the contrasting root distributions shown in Figure 4a, rather than a validated soil C-retention threshold (Fonta et al., 2022; Henry et al., 2011; Oo et al., 2025).

Source-maximizer. Sustained assimilate supply during grain filling is evaluated using repeated photosynthesis measurements together with post-heading dry-mass gain. SLA, flag-leaf dimensions, and upper-leaf angle help interpret that performance alongside LAI and canopy light distribution

(Figure 4b), rather than serving as independent selection maxima (Burgess et al., 2017; Fukuda et al., 2025; Lin et al., 2026). In an irrigated field panel of 318 *indica* accessions at Los Baños during the 2016 dry season, flag-leaf length ranged from 20.3 to 49.5 cm and width from 0.86 to 2.40 cm at seven days after anthesis (H.-C. Lin et al., 2026). The field comparison of CSSLs in Table 6 provides one measured contrast in photosynthetic performance, rather than a universal target (Ni et al., 2026).

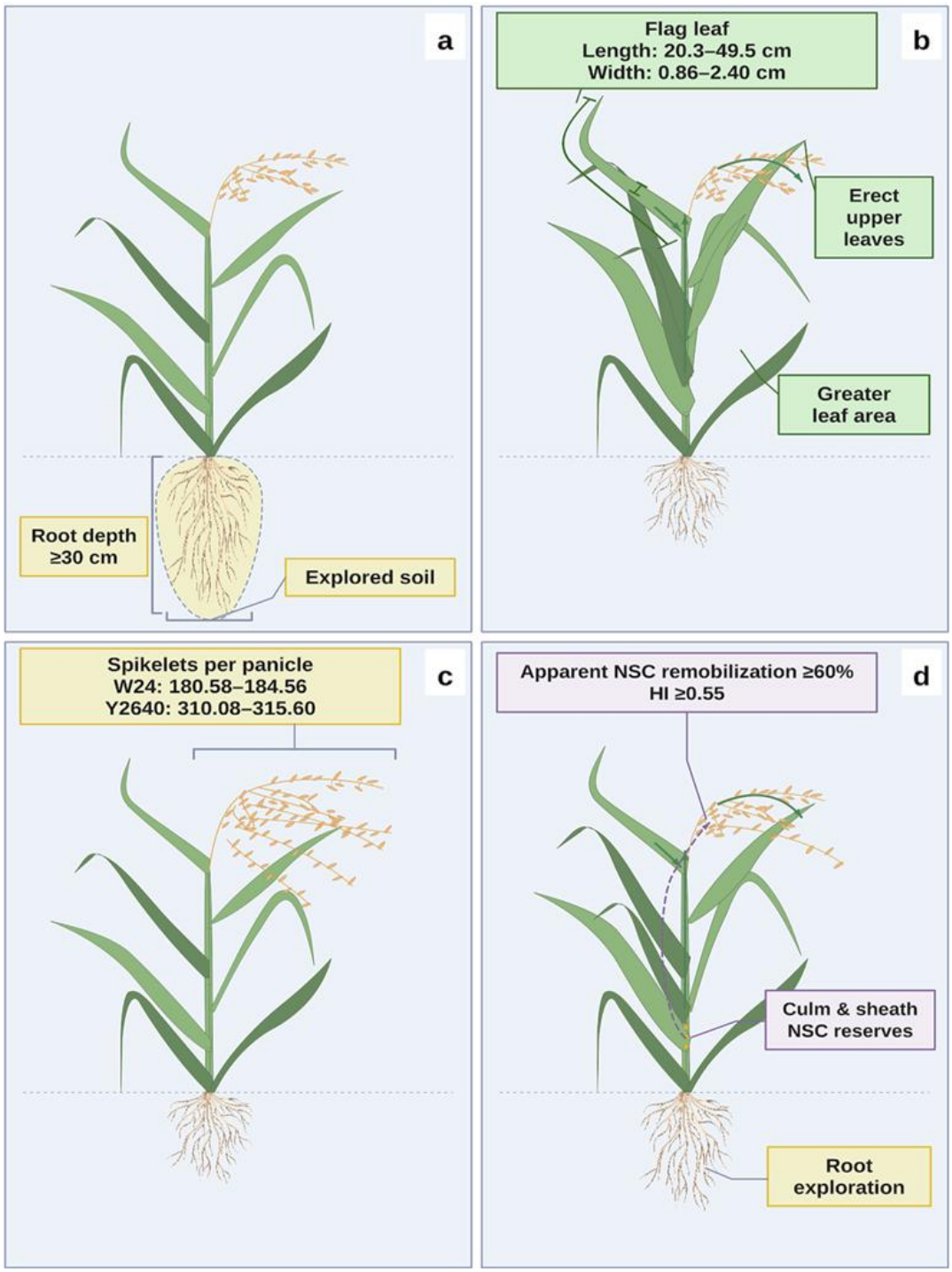


Figure 4. Root, source, and sink traits in four candidate rice archetypes. (a) Deep-explorer: deeper subsoil exploration. (b) Source-maximizer: greater leaf area and erect upper leaves. (c) Sink-maximizer: larger potential grain sink. (d) Balanced-integrator: coordinated acquisition, assimilation, and reserve export with maintained grain yield. Brackets indicate structural extent; panels are not to scale. Flag-leaf ranges are from indica accessions (Lin et al., 2026); spikelet ranges compare Wuyunjing 24 (W24) and Yongyou 2640 (Y2640) (Zang et al., 2024). Thresholds are proposed screening criteria (Table 6). Green arrows indicate current assimilate supply; purple arrows indicate export of culm and leaf-sheath NSC reserves (gold circles). (Adapted from artwork created with BioRender.com).

Table 6
Candidate rice archetypes: proposed criteria and illustrative observations

Archetype	Priority measurements	Proposed criterion	Illustrative observation (source)
Deep-explorer	Depth (cm); subsoil root fraction (%); RLD (cm cm^{-3}).	Depth ≥30 cm and greater subsoil RLD or fraction than the reference.	Root-mass fraction, 10–30/0–30 cm: Dro1-NIL 15%, IR64 9%, qsor1-NIL 4%; flooded P-dipping + N, 60 DAT (Oo et al., 2025).
Source-maximizer	Repeated net assimilation; post-heading biomass gain; canopy traits (Table 3).	Greater sustained assimilate supply; do not maximize SLA or LAI alone.	Peak assimilation in CSSL #91 was 12.8–18.3% above #19; Yangzhou, 0/120/240 kg N ha^{-1} (Ni et al., 2026).
Sink-maximizer	Panicle density; spikelets per panicle; potential grain mass; filled grains (%).	Greater potential sink per ground area, with maintained or improved filling.	180.58–184.56 spikelets $panicle^{-1}$ in Wuyunjing 24 versus 310.08–315.60 in Yongyou 2640; well-watered/AWMD, 270 kg N ha^{-1} (Zang et al., 2024).
Balanced-integrator	Apparent NSC remobilization (% of heading pool); HI; yield; biomass gain.	NSC remobilization ≥60% and HI ≥0.55, with maintained grain yield.	Remobilization: well-watered 24.4–35.0%; AWMD 59.7–68.9% (Zang et al., 2024). HI in CSSL #91: 0.4330–0.5682 (Ni et al., 2026; Table 3).

Note. Criteria are author-proposed and must be tested jointly with yield and C outcomes. Comparisons require a prespecified reference and matched water regime, stage and management. DAT, days after transplanting; RLD, root length density; NSC, non-structural carbohydrates; HI, harvest index; SLA, specific leaf area; LAI, leaf area index; CSSL, chromosome single-segment substitution line; AWMD, alternate wetting and moderate drying. Additional values: Table S8 (Supplementary Material).

Sink-maximizer. Greater potential grain capacity per ground area is evaluated from panicle density, spikelets per panicle, and potential grain mass (Figure 4c). Whether that capacity is realized is assessed through filled-grain percentage and grain-growth trajectories, with carbohydrate transport and starch-deposition activity characterizing sink utilization (Ni et al., 2026; Paul et al., 2017; Tu et al., 2022; Zang et al., 2024). Assignment therefore requires evidence of grain filling, not panicle size alone.

Balanced-integrator. This profile coordinates root acquisition and current assimilation with grain demand and reserve export from culms and leaf sheaths (Figure 4d). As provisional joint screening criteria, we propose apparent NSC remobilization ≥60% and HI ≥0.55 without a reduction in grain yield; post-heading biomass gain and grain-filling trajectories are used to assess that coordination (Ni et al., 2026; Yang & Zhang, 2010; Zang et al., 2024). The proposed profiles must now be evaluated against trade-offs among carbon allocation, soil C persistence, and methane emissions, which vary with water regime and management.

7. Current and future challenges

Carbon gain, carbon retention, and methane mitigation do not necessarily converge within the same phenotype, because root-derived inputs can stimulate rhizosphere turnover and alter gaseous losses under flooded conditions (Dijkstra et al., 2021; Kimura et al., 2004; Liu et al., 2019). Greater allocation to harvestable biomass may reduce the fraction of fixed carbon returned to soil even when yield increases (Fageria, 2007; Liu et al., 2019; Zhang et al., 2017). Assessing the climatic value of these traits requires integrating carbon allocation, residue fate, soil stabilization, and gaseous emissions (Cheng & Kuzyakov, 2005; Mandal et al., 2021; Pu et al., 2021; Tang et al., 2019). In coastal Indian rice-based systems, positive net ecosystem carbon balances coexisted with net greenhouse-gas emissions, with reduced tillage and residue retention providing an exception in the management treatments studied (Mandal et al., 2021).

The aerenchyma relationships summarized in Table 2 illustrate how irrigation can change the direction of a trait–CH_4 association (Li et al., 2025). In field experiments with six cultivars at Yangzhou and Zhenjiang in 2019 – 2020, the group with more developed aerenchyma emitted less CH_4 under continuous flooding but 28% – 32% more under alternate wetting and drying than the group with less developed aerenchyma (Li et al., 2025). Both regimes received 270 kg N ha^{-1}; the drying treatment was reirrigated at −15 kPa at a soil depth of 15 – 20 cm (Li et al., 2025). Greater root oxygen release supported the oxidation mechanism proposed for continuous flooding, whereas enhanced transport from deeper anaerobic soil was proposed to explain the higher emissions under alternate wetting and drying (Li et al., 2025).

Developmental stage also changes the relationships between canopy traits and CH_4 emissions (Fang et al., 2026). Across two field seasons in Anhui, high-yield, low-emitting cultivars had lower LAI, tiller number, and SPAD at tillering than low-yield, high-emitting cultivars, but higher aboveground trait values at heading except for tiller number (Fang et al., 2026). Path modeling showed that aboveground traits were positively associated with CH_4 at tillering, while root traits were negatively associated with CH_4 at heading (Fang et al., 2026). These cultivar contrasts were obtained under flooding with midseason aeration and different N rates for indica and japonica, 240 and 280 kg N ha^{-1}, respectively (Fang et al., 2026).

Carbon partitioning provides a further trade-off between grain production and substrate supply to methanogens (Zou et al., 2026). In pot experiments with Yongyou 1540, $^{13}CO_2$ pulse labeling showed that ratoon rice allocated more newly fixed carbon to grain and less to rhizosphere soil than main-crop or late rice, with lower production of labeled CH_4 (Zou et al., 2026). Related exudate analyses found less acetate in ratoon rice (Zou et al., 2026). The accompanying two-year field comparisons also recorded lower daily CH_4 emissions in ratoon rice, although crop duration and N supply differed among cropping regimes (Zou et al., 2026).

Exudate composition and microbial metabolism add another dimension to these plant traits (Shi et al., 2026). In flooded greenhouse pots, Kitaake lines overexpressing OsPSY1 or OsPSY2 emitted less cumulative CH_4 over 70 days than wild-type controls (Shi et al., 2026). Rhizosphere metatranscriptomics detected higher transcriptional activity of bacterial H_2-oxidation pathways, while metabolic modeling predicted less H_2 available for hydrogenotrophic methanogenesis (Shi et al., 2026). Altered root exudate chemistry may explain these microbial responses (Shi et al., 2026).

Whether a genotype retains its functional profile across aerobic, flooded, and AWD conditions remains a validation question. Root architecture varies with genotype and water supply (Bañoc et al., 2000a, 2000b; Gu et al., 2017; Kato et al., 2013; Mishra & Salokhe, 2011; Phule et al., 2019), as do biomass partitioning, harvest index and source–sink synchrony (Fageria, 2007; Mohapatra et al., 2011; Tu et al., 2022; Vishwakarma et al., 2024; Yang & Zhang, 2023). Field comparisons should therefore separate within-genotype plasticity from repeatable trait–outcome associations at matched developmental stages and under clearly specified water regimes.

8. Conclusions

We hypothesize that combining deep-explorer root traits with balanced-integrator source–sink function could improve seasonal carbon balance without reducing grain yield, but this combined performance has not been validated in the field. Greater carbon uptake or root biomass alone cannot establish persistent carbon retention soil or a favorable greenhouse-gas balance.

A minimum viable field test would evaluate eight genotypes, including a prespecified reference and candidates expressing the combined profile, at one site during one rice-growing season. In three blocks, hydraulically isolated, independently irrigated main plots would receive aerobic irrigation, continuous flooding, or alternate wetting and drying (AWD); eight genotypes would be randomized as subplots (nine irrigation units and 72 genotype subplots). Aerobic soil would remain nonflooded and below saturation, with nitrogen supply, planting density, and residue management held constant. Water-regime effects would be tested using the main-plot error term; three blocks would provide a pilot assessment rather than definitive threshold validation.

At matched developmental stages, measurements would include root architecture and root:shoot biomass allocation, organ C concentrations, net photosynthesis, reserve remobilization, grain filling, grain yield, and harvested C exports. Daytime and nighttime measurements of net ecosystem CO_2 exchange, CH_4 and N_2O fluxes, along with event-focused and waterborne C sampling, would support separate seasonal C and CO_2-equivalent balances, avoiding conflation of methane-C accounting with CH_4 warming effects.

Soil sampling before planting and after harvest would cover the proposed 0 – 20 and 20 – 40 cm layers, extending deeper where necessary, with stock comparisons based on equivalent soil mass and measured bulk density. The trial would estimate yield, seasonal net ecosystem carbon balance, and greenhouse-gas responses within each water regime, reporting genotype × regime interactions and uncertainty. Multiyear, multisite validation with repeated soil-stock measurements would still be needed to test archetype stability, proposed thresholds, and persistent soil C retention before deployment in breeding programs.

Financial interests: Author Angélica Alejandra Palma Araúz received funding for tuition and living expenses from SENACYT-IFARHU (Secretaría Nacional de Ciencia, Tecnología e Innovación-Instituto para la Formación y Aprovechamiento de los Recursos Humanos, Panama) under contract number 270-2023-008.

Non-financial interests: none.

Ethics approval: Not applicable. This article is a review of previously published literature and does not contain any studies with human participants or animals performed by the authors.

Consent to participate: Not applicable. This study did not involve human participants.

Consent for publication: Not applicable. This article does not include any individual person's data in any form (including individual details, images or videos).

Data availability: Data sharing is not applicable to this article as no datasets were generated or analyzed during the current study.

Authors' contributions

A. A. Palma-Araúz: conceptualization, investigation, data curation, formal analysis, writing original draft. **M. A. García Dávila** and **M. A. Caicedo-Baltodano**: conceptualization, writing, review and editing.

ORCID

A. A. Palma-Araúz https://orcid.org/0000-0003-2095-6168
M. A. García Dávila https://orcid.org/0000-0001-8197-6344
M. A. Caicedo-Baltodano https://orcid.org/0000-0002-6517-1471

References

Anilkumar, C., & Bernardo, R. (2026). Genomewide selection in rice (*Oryza sativa* L.) breeding: Balancing cost and time for higher genetic gain. *Plant Breeding*, *145*(2), 298–305. https://doi.org/10.1111/pbr.70042

Aulakh, M. S., Bodenbender, J., Wassmann, R., & Rennenberg, H. (2000). Methane transport capacity of rice plants. II. Variations among different rice cultivars and relationship with morphological characteristics. *Nutrient Cycling in Agroecosystems*, *58*, 367-375. https://doi.org/10.1023/A:1009839929441

Bañoc, D. M., Yamauchi, A., Kamoshita, A., Wade, L., & Pardales, J. (2000a). Dry matter production and root system development of rice cultivars under fluctuating soil moisture. *Plant Production Science*, *3*(2), 197-207. https://doi.org/10.1626/pps.3.197

Bañoc, D. M., Yamauchi, A., Kamoshita, A., Wade, L., & Pardales, J. (2000b). Genotypic variations in response of lateral root development to fluctuating soil moisture in rice. *Plant Production Science*, *3*(3), 335-343. https://doi.org/10.1626/pps.3.335

Bellini, C., Pacurar, D. I., & Perrone, I. (2014). Adventitious roots and lateral roots: Similarities and differences. *Annual Review of Plant Biology, 65,* 639-666. https://doi.org/10.1146/annurev-arplant-050213-035645

Brüggemann, N., Gessler, A., Kayler, Z., Keel, S. G., Badeck, F., Barthel, M., et al. (2011). Carbon allocation and carbon isotope fluxes in the plant-soil-atmosphere continuum: A review. *Biogeosciences*, *8*(11), 3457–3489. https://doi.org/10.5194/bg-8-3457-2011

Bueno, C. S., & Lafarge, T. (2009). Higher crop performance of rice hybrids than of elite inbreds in the tropics: 1. Hybrids accumulate more biomass during each phenological phase. *Field Crops Research*, *112*(2–3), 229–237. https://doi.org/10.1016/j.fcr.2009.03.006

Burgess, A. J., Retkute, R., Herman, T., & Murchie, E. H. (2017). Exploring relationships between canopy architecture, light distribution, and photosynthesis in contrasting rice genotypes using 3D canopy reconstruction. *Frontiers in Plant Science*, 8, 734. https://doi.org/10.3389/fpls.2017.00734

Chauhan, B. S., Jabran, K., & Mahajan, G. (Eds.). (2017). *Rice Production Worldwide*. Springer International Publishing, Switzerland. https://doi.org/10.1007/978-3-319-47516-5

Chawade, A., Van Ham, J., Blomquist, H., Bagge, O., Alexandersson, E., & Ortiz, R. (2019). High-throughput field-phenotyping tools for plant breeding and precision agriculture. *Agronomy*, *9*(5), 258. https://doi.org/10.3390/agronomy9050258

Chen, T., Yang, X., Fu, W., Li, G., Feng, B., Fu, G., & Tao, L. (2022). Strengthened assimilate transport improves yield and quality of super rice. *Agronomy*, *12*(4), 753. https://doi.org/10.3390/agronomy12040753

Chen, Y. L., & Rengel, Z. (2015). Phenotyping for root traits. In *Phenomics in Crop Plants: Trends, Options and Limitations* (pp. 101–128). Springer India. https://doi.org/10.1007/978-81-322-2226-2_8

Cheng, W., & Kuzyakov, Y. (2005). Root effects on soil organic matter decomposition. In R. W. Zobel & S. F. Wright (Eds.), *Roots and Soil Management: Interactions between Roots and the Soil* (Vol. 48, pp. 119–143). John Wiley & Sons, Ltd. https://doi.org/10.2134/agronmonogr48.c7

Colmer, T. D. (2003a). Aerenchyma and an inducible barrier to radial oxygen loss facilitate root aeration in upland, paddy and deep-water rice (*Oryza sativa* L.). *Annals of Botany*, *91*, 301–309. https://doi.org/10.1093/aob/mcf114

Colmer, T. D. (2003b). Long-distance transport of gases in plants: a perspective on internal aeration and radial oxygen loss from roots. *Plant, Cell & Environment*, *26*, 17–36. https://doi.org/10.1046/j.1365-3040.2003.00846.x

Colmer, T. D., & Pedersen, O. (2008). Oxygen dynamics in submerged rice (Oryza sativa). *New Phytologist*, *178*(2), 326–334. https://doi.org/10.1111/j.1469-8137.2007.02364.x

Colmer, T. D., & Voesenek, L. A. C. J. (2009). Flooding tolerance: suites of plant traits in variable environments. *Functional Plant Biology*, *36*, 665–681. https://doi.org/10.1071/fp09144

Core Writing Team, Lee, H., & Romero, J. (Eds.). (2023). *IPCC, 2023: Climate Change 2023: Synthesis Report. Contribution of Working Groups I, II and III to the Sixth Assessment Report of the Intergovernmental Panel on Climate Change.* IPCC. https://doi.org/10.59327/IPCC/AR6-9789291691647

Das, S. R., Nayak, B. K., Dey, S., Sarkar, S., Chatterjee, D., Saha, S., Sarkar, D., Pradhan, A., Saha, S., & Nayak, A. K. (2023). Potential soil organic carbon sequestration vis-a-vis methane emission in lowland rice agroecosystem. *Environmental Monitoring and Assessment, 195*(9). https://doi.org/10.1007/s10661-023-11673-0

Deng, Z., Chen, J., Wang, S., Li, T., Huang, K., Gu, P., Peng, H., & Chen, Z. (2025). Response of vegetation photosynthesis to the 2022 drought in Yangtze River Basin by diurnal Orbiting Carbon Observatory-2/3 satellite observations. *Journal of Remote Sensing, 5*,0445. https://doi.org/10.34133/remotesensing.0445

Dijkstra, F. A., Zhu, B., & Cheng, W. (2021). Root effects on soil organic carbon: a double-edged sword. *New Phytologist, 230*(1), 60-65. https://doi.org/10.1111/nph.17082

Ding, H., Jiang, Y., & Cao, C. (2021). Deep rice root systems reduce methane emissions in rice paddies. *Plant and Soil, 468,* 337-352. https://doi.org/10.1007/s11104-021-05118-1

Dinh, L. T., Pandey, B. K., Ueda, Y., Leftley, N., Atkinson, B. S., Bennett, M. J., & Wissuwa, M. (2026). Quantitative trait locus qLDC5 regulates primary root branching in an auxin-dependent manner. *Journal of Experimental Botany, 77*(17), 5639–5650. https://doi.org/10.1093/jxb/erag232

Fageria, N. K. (2007). Yield physiology of rice. *Journal of Plant Nutrition*, *30*(6), 843-879. https://doi.org/10.1080/15226510701374831

Falqueto, A. R., Silva, F. S. P., Cassol, D., Magalhães, A. M., Oliveira, A. C., & Bacarin, M. A. (2010). Chlorophyll fluorescence in rice: probing of senescence driven changes of PSII activity on rice varieties differing in grain yield capacity. *Brazilian Journal of Plant Physiology, 22*(1), 35–41. https://doi.org/10.1590/S1677-04202010000100004

Fang, S., Yu, N., Zhu, W., Yin, C., Ma, T., Zhu, T., You, C., He, H., Zhang, Q., Xu, C., Wu, L., & Ke, J. (2026). Stage-specific drivers of double-peak methane mitigation in paddy fields with high-yield rice varieties. *Field Crops Research*, 346, 110603. https://doi.org/10.1016/j.fcr.2026.110603

Fei, C., Geng, X., Xu, Z., & Xu, Q. (2019). Multiple areas investigation reveals the genes related to vascular bundles in rice. *Rice, 12*(17). https://doi.org/10.1186/s12284-019-0278-x

Ferguson, J. N., Mcausland, L., Smith, K. E., Price, A., Wilson, Z., & Murchie, E. (2020). Rapid temperature responses of photosystem II efficiency forecast genotypic variation in rice vegetative heat tolerance. *The Plant Journal*, *104*(3), 839-855. https://doi.org/10.1111/tpj.14956

Fonta, J. E., Vejchasarn, P., Henry, A., Lynch, J., & Brown, K. (2022). Many paths to one goal: Identifying integrated rice root phenotypes for diverse drought environments. *Frontiers in Plant Science, 13,* 959629. https://doi.org/10.3389/fpls.2022.959629

Freschet, G. T., Pagès, L., Iversen, C. M., Comas, L. H., Rewald, B., Roumet, C., et al. (2021a). A starting guide to root ecology: strengthening ecological concepts and standardising root

classification, sampling, processing and trait measurements. *New Phytologist*, *232*(3), 973–1122. https://doi.org/10.1111/nph.17572

Freschet, G. T., Roumet, C., Comas, L. H., Weemstra, M., Bengough, A. G., Rewald, B., et al. (2021b). Root traits as drivers of plant and ecosystem functioning: current understanding, pitfalls and future research needs. *New Phytologist*, 232(3), 1123–1158. https://doi.org/10.1111/nph.17072

Fu, P., Montes, C. M., Siebers, M. H., Gómez-Casanovas, N., McGrath, J., Ainsworth, E., & Bernacchi, C. (2022). Advances in field-based high-throughput photosynthetic phenotyping. *Journal of Experimental Botany, 73*(10), 3157-3172. https://doi.org/10.1093/jxb/erac077

Fukuda, S., Okamura, M., & Sugiura, D. (2025). Non-destructive estimation of rice canopy LAI using NIR/PAR: application to four rice cultivars with diverse leaf characteristics and plant architectures. *Discover Agriculture*, 3, 153. https://doi.org/10.1007/s44279-025-00343-z

Furbank, R. T., & Tester, M. (2011). Phenomics – technologies to relieve the phenotyping bottleneck. *Trends in Plant Science*, *16*(12), 635–644. https://doi.org/10.1016/j.tplants.2011.09.005

Gangopadhyay, S., Banerjee, R., Batabyal, S., Das, N., Mondal, A., Pal, S., & Mandal, S. (2022). Carbon sequestration and greenhouse gas emissions for different rice cultivation practices. *Sustainable Production and Consumption*, *34*, 90-104. https://doi.org/10.1016/j.spc.2022.09.001

Gu, D., Zhen, F., Hannaway, D. B., Zhu, Y., Liu, L., Cao, W., & Tang, L. (2017). Quantitative classification of rice (*Oryza sativa* L.) root length and diameter using image analysis. *PLoS ONE*, *12*(1), e0169968. https://doi.org/10.1371/journal.pone.0169968

Guimarães, P. H. R., Pereira de Lima, I., Pereira de Castro, A., Lanna, A. C., Guimarães Santos Melo, P., & de Raïssac, M. (2020). Phenotyping root systems in a set of japonica rice accessions: Can structural traits predict the response to drought? *Rice, 13*, 67.https://doi.org/10.1186/s12284-020-00404-5

Gul, S., & Whalen, J. (2013). Plant life history and residue chemistry influences emissions of CO2 and N2O from soil: Perspectives for genetically modified cell wall mutants. *Critical Reviews in Plant Sciences*, *32*(5), 344–368. https://doi.org/10.1080/07352689.2013.781455

Guo, Y., & Lv, Y. (2025). Evaluation of models for describing photosynthetic light–response curves and estimating parameters in rice leaves at various canopy positions. *Agronomy*, *15*(1), 125. https://doi.org/10.3390/agronomy15010125

Haque, M. M., Biswas, J. C., Hwang, H. Y., & Kim, P. J. (2020). Annual net carbon budget in rice soil. *Nutrient Cycling in Agroecosystems*, *116*, 31-40. https://doi.org/10.1007/s10705-019-10029-w

Henry, A., Gowda, V. R. P., Torres, R. O., McNally, K. L., & Serraj, R. (2011). Variation in root system architecture and drought response in rice (Oryza sativa): Phenotyping of the OryzaSNP panel in rainfed lowland fields. *Field Crops Research*, *120*, 205–214. https://doi.org/10.1016/j.fcr.2010.10.003

Henry, A., Cal, A. J., Batoto, T. C., Torres, R., & Serraj, R. (2012). Root attributes affecting water uptake of rice (*Oryza sativa* L.) under drought. *Journal of Experimental Botany, 63*(13), 4751-4763. https://doi.org/10.1093/jxb/ers150

Hinsinger, P., Bengough, A. G., Vetterlein, D., & Young, I. M. (2009). Rhizosphere: biophysics, biogeochemistry and ecological relevance. *Plant and Soil*, *321*, 117–152. https://doi.org/10.1007/s11104-008-9885-9

Hirayama, M., Wada, Y., & Nemoto, H. (2006). Estimation of drought tolerance based on leaf temperature in upland rice breeding. *Breeding Science, 56*, 47–54. https://doi.org/10.1270/jsbbs.56.47

Hodge, A., Berta, G., Doussan, C., Merchan, F., & Crespi, M. (2009). Plant root growth, architecture and function. *Plant Soil*, *321*, 153-187. https://doi.org/10.1007/s11104-009-9929-9

Horii, H., Nemoto, K., Miyamoto, N., & Harada, J. (2006). Quantitative trait loci for adventitious and lateral roots in rice. *Plant Breeding*, *125*(2), 198–200. https://doi.org/10.1111/j.1439-0523.2006.01124.x

Hossain, M. L., & Li, J. (2021). Biomass partitioning of C_3- and C_4-dominated grasslands in response to climatic variability and climate extremes. *Environmental Research Letters*, *16*, 074016. https://doi.org/10.1088/1748-9326/ac027a

Hou, L., Gao, W., van der Bom, F., Weng, Z., Doolette, C., Maksimenko, A., et al. (2022). Use of X-ray tomography for examining root architecture in soils. *Geoderma*, *405*, 115405. https://doi.org/10.1016/j.geoderma.2021.115405

Hussain, S., Peng, S., Fahad, S., Khaliq, A., Huang, J., Cui, K., & Nie, L. (2015). Rice management interventions to mitigate greenhouse gas emissions: a review. *Environmental Science and Pollution Research*, *22*, 3342-3360. https://doi.org/10.1007/s11356-014-3760-4

Iqbal, M. F., Liu, S., Zhu, J., Zhao, L., Qi, T., Liang, J., Luo, J., Xiao, X., & Fan, X. (2021). Limited aerenchyma reduces oxygen diffusion and methane emission in paddy. *Journal of Environmental Management*, *1*(279), 111583. https://doi.org/10.1016/j.jenvman.2020.111583

Jat, M. L., Dagar, J. C., Sapkota, T. B., Yadvinder-Singh, G. B., Ridaura, S., Saharawat, Y., et al. (2016). Climate change and agriculture: Adaptation strategies and mitigation opportunities for food security in South Asia and Latin America. In D. L. Sparks (Ed.) *Advances in Agronomy*. Academic Press Inc, pp. 127-235.https://doi.org/10.1016/bs.agron.2015.12.005

Ji, Y., Zhou, Y., Li, Z., Feng, K., Sun, X., Xu, Y., Wu, W., & Zou, H. (2024). Carbon footprint research and mitigation strategies for rice-cropping systems in China: a review. *Frontiers in Sustainable Food Systems*, *8*, 1375092. https://doi.org/10.3389/fsufs.2024.1375092

Jiménez, J de la C., & Pedersen, O. (2023). Mitigation of greenhouse gas emissions from rice via manipulation of key root traits. *Rice, 16*(24). https://doi.org/10.1186/s12284-023-00638-z

Jones, D. L., Nguyen, C., & Finlay, R. D. (2009a). Carbon flow in the rhizosphere: carbon trading at the soil–root interface. *Plant and Soil, 321*, 5–33. https://doi.org/10.1007/s11104-009-9925-0

Jones, H. G., Serraj, R., Loveys, B. R., Xiong, L., Wheaton, A., & Price, A. H. (2009b). Thermal infrared imaging of crop canopies for the remote diagnosis and quantification of plant responses to water stress in the field. *Functional Plant Biology, 36*(11), 978–989. https://doi.org/10.1071/fp09123

Kakar, N., Bheemanahalli, R., Jumaa, S., Redoña, E., Warburton, M., & Reddy, K. (2021). Assessment of agro-morphological, physiological and yield traits diversity among tropical rice. *PeerJ, 9*, e11752. https://doi.org/10.7717/peerj.11752

Kalaji, H. M., Schansker, G., Brestic, M., Bussotti, F., Calatayud, A., Ferroni, L., et al. (2017). Frequently asked questions about chlorophyll fluorescence, the sequel. In *Photosynthesis Research*, *132*, 13-66. https://doi.org/10.1007/s11120-016-0318-y

Kato, T., & Horibata, A. (2011). Non-random distribution of the alleles for good grain filling at OsAGPS2 and OsSUT1 among a wide range of rice (*Oryza sativa* L.) cultivars. *Breeding Science*, *61*(2), 217–220. https://doi.org/10.1270/jsbbs.61.217

Kato, Y., Tajima, R., Homma, K., Toriumi, A., Yamagishi, J., Shiraiwa, T., Mekwatanakarn, P., & Jongdee, B. (2013). Root growth response of rainfed lowland rice to aerobic conditions in northeastern Thailand. *Plant Soil, 368*, 557-567. https://doi.org/10.1007/s11104-012-1538-3

Kaya, C. (2025). Optimizing crop production with plant phenomics through high-throughput phenotyping and AI in controlled

environments. *Food and Energy Security*, *14*(1), e70050. https://doi.org/10.1002/fes3.70050

Kimura, M., Murase, J., & Lu, Y. (2004). Carbon cycling in rice field ecosystems in the context of input, decomposition and translocation of organic materials and the fates of their end products (CO_2 and CH_4). *Soil Biology and Biochemistry*, *36*(9), 1399-1416. https://doi.org/10.1016/j.soilbio.2004.03.006

Kingra, P. K., Kaur, R., & Kaur, S. (2019). Climate change impacts on rice (*Oryza sativa* L.) productivity and strategies for its sustainable management. *The Indian Journal of Agricultural Sciences*, *89*(2), 171-180. https://doi.org/10.56093/ijas.v89i2.86981

Kirk, G. J. D., Boghi, A., Affholder, M. C., Keyes, S. D., Heppell, J., & Roose, T. (2019). Soil carbon dioxide venting through rice roots. *Plant Cell and Environment*, *42*(12), 3197–3207. https://doi.org/10.1111/pce.13638

Kuzyakov, Y., & Domanski, G. (2000). Carbon input by plants into the soil. Review. *Journal of Plant Nutrition and Soil Science, 163*(4), 421-431. https://doi.org/10.1002/1522-2624(200008)163:4<421::AID-JPLN421>3.0.CO;2-R

Lafitte, H. R., Champoux, M. C., Mclaren, G., & O'Toole, J. C. (2001). Rice root morphological traits are related to isozyme group and adaptation. *Field Crops Research*, *71*(1), 57-70. https://doi.org/10.1016/S0378-4290(01)00150-2

Lal, R. (2004). Soil carbon sequestration impacts on global climate change and food security. *Science*, *304*(5677), 1623-1627. https://doi.org/10.1126/science.1097396

Lawson, T., & Blatt, M. R. (2014). Stomatal size, speed, and responsiveness impact on photosynthesis and water use efficiency. *Plant Physiology*, *164*(4), 1556-1570. https://doi.org/10.1104/pp.114.237107

Li, A., Zhu, L., Xu, W., Liu, L., & Teng, G. (2022). Recent advances in methods for in situ root phenotyping. *PeerJ*, *10*, e13638. https://doi.org/10.7717/peerj.13638

Li, G., Chen, X., Zhou, C., Yang, Z., Zhang, C., Huang, Z., Pan, W., & Xu, K. (2022). Vascular bundle characteristics of different rice variety treated with nitrogen fertilizers and its relation to stem assimilates allocation and grain yield. *Agriculture*, *12*(6), 779. https://doi.org/10.3390/agriculture12060779

Li, G., Hu, Q., Zhang, G., Shi, Y., Wang, W., Wang, Z., Xiong, D., Huang, J., Peng, S., & Cui, K. (2026). Sucrose unloading in grains modulates the disparity in grain filling of superior and inferior spikelets in rice. *Physiologia Plantarum*, 178, e70809. https://doi.org/10.1111/ppl.70809

Li, L., Zhang, Q., & Huang, D. (2014). A review of imaging techniques for plant phenotyping. *Sensors*, *14*(11), 20078–20111. https://doi.org/10.3390/s141120078

Li, S., Zhang, Y., Zhao, J., van Groenigen, K. J., Shen, X., Zhang, H., Gu, J., Zhang, W., Hui, D., Chen, Y., & Liu, L. (2025). Water-saving irrigation practices in rice paddies reverse the impact of root aerenchyma on methane emissions. *Agriculture, Ecosystems & Environment*, *378*, 109309. https://doi.org/10.1016/j.agee.2024.109309

Li, X., Yan, W., Agrama, H., Jia, L., Jackson, A., Moldenhauer, K., Yeater, K., McClung, A., & Wu, D. (2012). Unraveling the complex trait of harvest index with association mapping in rice (*Oryza sativa* L.). *PLOS ONE*, *7*(1), e29350. https://doi.org/10.1371/journal.pone.0029350

Liao, S., Yan, J., Xing, H., Tu, Y., Zhao, H., & Wang, G. (2021). Genetic basis of vascular bundle variations in rice revealed by genome-wide association study. *Plant Science, 302*, 110715. https://doi.org/10.1016/j.plantsci.2020.110715

Lin, C., Zhu, T., Ogorek, L. L. P., Wang, Y., Sauter, M., & Pedersen, O. (2022). The pyramiding of three key root traits aid breeding of flood-tolerant rice. *Plants*, *11*(15). https://doi.org/10.3390/plants11152033

Lin, H.-C., Dionora, J., Chebotarov, D., Laza, M. R., Naredo, M. E. B., Muyco, P. A., et al. (2026). Diversity of photosynthesis-related and high-throughput phenotyping traits in *indica* rice. *Current Plant Biology*, 47, 100613. https://doi.org/10.1016/j.cpb.2026.100613

Liu, Q., Chen, S., Zhou, L., Tao, Y., Tian, J., Xing, Z., Wei, H., & Zhang, H. (2022). Characteristics of population quality and rice quality of semi-waxy japonica rice varieties with different grain yields. *Agriculture*, *12*(2), 241. https://doi.org/10.3390/agriculture12020241

Liu, S., Xiong, Z., Zhang, Z., Wei, Y., Xiong, D., Wang, F., & Huang, J. (2023). Exploration of chlorophyll fluorescence characteristics gene regulatory in rice (*Oryza sativa* L.): a genome-wide association study. *Frontiers in Plant Science*, *14*, 1234866. https://doi.org/10.3389/fpls.2023.1234866

Liu, Y., Ge, T., Zhu, Z., Liu, S., Luo, Y., Li, Y., Wang, P., et al. (2019). Carbon input and allocation by rice into paddy soils: A review. *Soil Biology and Biochemistry*, *133*, 97-107. https://doi.org/10.1016/j.soilbio.2019.02.019

Lu, B. R., Cai, X., & Jin, X. (2009). Efficient indica and japonica rice identification based on the InDel molecular method: Its implication in rice breeding and evolutionary research. *Progress in Natural Science*, *19*(10), 1241-1252. https://doi.org/10.1016/j.pnsc.2009.01.011

Lu, Y., Watanabe, A., & Kimura, M. (2003). Carbon dynamics of rhizodeposits, root- and shoot-residues in a rice soil. *Soil Biology and Biochemistry*, *35*(9), 1223–1230. https://doi.org/10.1016/S0038-0717(03)00184-6

Luan, Y., Xu, J., Lv, Y., Liu, X., Wang, H., & Liu, S. (2021). Improving the performance in crop water deficit diagnosis with canopy temperature spatial distribution information measured by thermal imaging. *Agricultural Water Management*, *246*, 106699. https://doi.org/10.1016/j.agwat.2020.106699

Lynch, J. P. (2007). Roots of the second green revolution. *Australian Journal of Botany*, *55*(5), 493–512. https://doi.org/10.1071/bt06118

Mandal, U. K., Bhardwaj, A. K., Lama, T. D., Nayak, D. B., Samui, A., Burman, D., Mahanta, K. K., Sarangi, S. K., Mandal, S., & Raut, S. (2021). Net ecosystem exchange of carbon, greenhouse gases, and energy budget in coastal lowland double cropped rice ecology. *Soil and Tillage Research*, *212*, 105076. https://doi.org/10.1016/j.still.2021.105076

Mao, T., Xu, H., Xu, Q., Guo, Y., Zhu, C., Chen, K., Wang, J., & Xu, Z. (2010). Comparison of morphological and genetic differentiations in filial generation of cross between indica and japonica rice. *Rice Science, 17*(1), 82-86. https://doi.org/10.1016/S1672-6308(08)60108-0

Maqbool, S., Hassan, M. A., Xia, X., York, L., Rasheed, A., & He, Z. (2022). Root system architecture in cereals: progress, challenges and perspective. *The Plant Journal*, *110*(1), 23–42. https://doi.org/10.1111/tpj.15669

Mayanja, I. K., Diepenbrock, C. H., Vadez, V., Lei, T., & Bailey, B. N. (2024). Practical considerations and limitations of using leaf and canopy temperature measurements as a stomatal conductance proxy: Sensitivity across environmental conditions, scale, and sample size. *Plant Phenomics*, *6*, 0169. https://doi.org/10.34133/plantphenomics.0169

Mertens, S., Verbraeken, L., Sprenger, H., De Meyer, S., Demuynck, K., Cannoot, B., et al. (2023). Monitoring of drought stress and transpiration rate using proximal thermal and hyperspectral imaging in an indoor automated plant phenotyping platform. *Plant Methods*, *19*(132). https://doi.org/10.1186/s13007-023-01102-1

Mi, W., Yang, B., Guo, S., Gao, F., Zhu, K., & Chen, S. (2026). Growth stage mediates the effects of water regime and long-term fertilization on carbon partitioning in the rice–rhizosphere system. *Plant and Soil, 525*, 1589–1601. https://doi.org/10.1007/s11104-026-08849-1

Mishra, A., & Salokhe, V. M. (2011). Rice root growth and physiological responses to SRI water management and implications for crop productivity. *Paddy Water Environment, 9,* 41–52. https://doi.org/10.1007/s10333-010-0240-4

Mohammed, G. H., Colombo, R., Middleton, E. M., Rascher, U., van der Tol, C., et al. (2019). Remote sensing of solar-induced chlorophyll fluorescence (SIF) in vegetation: 50 years of progress. *Remote Sensing of Environment, 231*, 111177. https://doi.org/10.1016/j.rse.2019.04.030

Mohapatra, P. K., Panigrahi, R., & Turner, N. C. (2011). Physiology of Spikelet Development on the Rice Panicle: Is Manipulation of Apical Dominance Crucial for Grain Yield Improvement? In: *Advances in Agronomy*. Elsevier Inc., pp. 333-359. https://doi.org/10.1016/b978-0-12-385531-2.00005-0

Mohapatra, P. K., & Sahu, B. B. (2021). Panicle Architecture of Rice and its Relationship with Grain Filling. In*: Panicle Architecture of Rice and its Relationship with Grain Filling*. Springer International Publishing, Switzerland. https://doi.org/10.1007/978-3-030-67897-5

Moradi, F., & Ismail, A. M. (2007). Responses of photosynthesis, chlorophyll fluorescence and ROS-scavenging systems to salt stress during seedling and reproductive stages in rice. *Annals of Botany, 99*(6), 1161-1173. https://doi.org/10.1093/aob/mcm052

Nguyen, V. N. T., Moon, S., Koh, H. J., Nguyen, Q. N., Yoon, B. S., Kim, B., Koh, H. J., & Jung, K. H. (2015). Genome-wide transcriptome comparison of flag leaves among japonica and indica varieties. *Journal of Plant Biology*, *58*(5), 333–343. https://doi.org/10.1007/s12374-015-0333-0

Ni, C., Zhang, J., Zhu, C., Hu, Q., Huo, Z., Dai, Q., Xu, K., & Li, G. (2026). Sucrose metabolism and translocation regulate stem–grain biomass partitioning to enhance grain yield in rice. *Field Crops Research*, 342, 110457. https://doi.org/10.1016/j.fcr.2026.110457

Ohsumi, A., Hamasaki, A., Nakagawa, H., Homma, K., Horie, T., & Shiraiwa, T. (2008). Response of leaf photosynthesis to vapor pressure difference in rice (*Oryza sativa* L.) varieties in relation to stomatal and leaf internal conductance. *Plant Production Science, 11*(2), 184-191. https://doi.org/10.1626/pps.11.184

Oo, A. Z., Tsujimoto, Y., Ranjakason, M. N. A., Andrianary, B. H., Raharinivo, V., Takai, T., & Uga, Y. (2025). Shallow root system with a DRO1 homolog combined with localized P application via P-dipping improves P use efficiency for rice production in nutrient-deficient lowlands in Madagascar. *Field Crops Research*, *331*, 110008. https://doi.org/10.1016/j.fcr.2025.110008

Oue, H. (2023). Comparisons of the stomatal conductance and electron transport rate of three Japanese rice cultivars including Himenorin in Ehime Prefecture. *Journal of Agricultural Meteorology*, *79*(2), 77–84. https://doi.org/10.2480/agrmet.D-22-00025

Ouyang, W., Struik, P. C., Yin, X., & Yang, J. (2017). Stomatal conductance, mesophyll conductance, and transpiration efficiency in relation to leaf anatomy in rice and wheat genotypes under drought. *Journal of Experimental Botany, 68*(18), 5191-5205. https://doi.org/10.1093/jxb/erx314

Paez-Garcia, A., Motes, C. M., Scheible, W.-R., Chen, R., Blancaflor, E. B., & Monteros, M. J. (2015). Root traits and phenotyping strategies for plant improvement. *Plants*, *4*, 334–355. https://doi.org/10.3390/plants4020334

Park, H. J., Lim, S. S., Kwak, J. H., Lee, K. S., In Yang, H., Kim, H. Y., Lee, S. M., & Choi, W. J. (2020). Biomass, chemical composition, and microbial decomposability of rice root and straw produced under co-elevated CO_2 and temperature. *Biology and Fertility of Soils, 56*, 991–1005. https://doi.org/10.1007/S00374-020-01471-y

Paul, M. J., Oszvald, M., Jesus, C., Rajulu, C., Griffiths, C. A., & Raines, C. (2017). Increasing crop yield and resilience with trehalose 6-phosphate: targeting a feast-famine mechanism in cereals for better source-sink optimization. *Journal of Experimental Botany, 68*(16), 4455– 4462. https://doi.org/10.1093/jxb/erx083

Pausch, J., & Kuzyakov, Y. (2018). Carbon input by roots into the soil: Quantification of rhizodeposition from root to ecosystem scale. *Global Change Biology*, *24*(1), 1–12. https://doi.org/10.1111/gcb.13850

Phule, A. S., Barbadikar, K. M., Madhav, M. S., Subrahmanyam, D., Senguttuvel, P., Babu, M. B. B. P., & Kumar, P. A. (2019). Studies on root anatomy, morphology and physiology of rice grown under aerobic and anaerobic conditions. *Physiology and Molecular Biology of Plants*, *25*(1), 197–205. https://doi.org/10.1007/s12298-018-0599-z

Pierret, A., Doussan, C., Capowiez, Y., Bastardie, F., & Pagès, L. (2007). Root functional architecture: A framework for modeling the interplay between roots and soil. *Vadose Zone Journal, 6*(2), 269–281. https://doi.org/10.2136/vzj2006.0067

Pierret, A., Maeght, J. L., Clément, C., Montoroi, J. P., Hartmann, C., & Gonkhamdee, S. (2016). Understanding deep roots and their functions in ecosystems: an advocacy for more unconventional research. *Annals of Botany*, *118*(4), 621–635. https://doi.org/10.1093/aob/mcw130

Pieruschka, R., & Schurr, U. (2019). Plant phenotyping: Past, present, and future. *Plant Phenomics*, *2019*, 7507131. https://doi.org/10.34133/2019/7507131

Poirier, V., Roumet, C., & Munson, A. D. (2018). The root of the matter: Linking root traits and soil organic matter stabilization processes. *Soil Biology and Biochemistry, 120*, 246-259. https://doi.org/10.1016/j.soilbio.2018.02.016

Pu, X., Dong, X., Cheng, H., Xie, J., Zhang, Y., Lu, L., Hu, Y., Song, W., & Xu, H. (2021). Dissolved organic carbon loss from paddy fields by drainage and roles of common ions. *Agriculture, Ecosystems and Environment, 307*, 107221. https://doi.org/10.1016/j.agee.2020.107221

Pump, J., & Conrad, R. (2014). Rice biomass production and carbon cycling in $13CO_2$ pulse-labeled microcosms with different soils under submerged conditions. *Plant and Soil*, *384*(1-2), 213-229. https://doi.org/10.1007/s11104-014-2201-y

Quero, G., Bonnecarrère, V., Fernández, S., Silva, P., Simondi, S., & Borsani, O. (2019). Light-use efficiency and energy partitioning in rice is cultivar dependent. *Photosynthesis Research, 140*(1), 51-63. https://doi.org/10.1007/s11120-018-0605-x

Rasse, D. P., Rumpel, C., & Dignac, M. F. (2005). Is soil carbon mostly root carbon? Mechanisms for a specific stabilisation. *Plant and Soil*, *269*, 341-356. https://doi.org/10.1007/s11104-004-0907-y

Reynolds, D., Baret, F., Welcker, C., Bostrom, A., Ball, J., Cellini, F., et al. (2019). What is cost-efficient phenotyping? Optimizing costs for different scenarios. *Plant Science, 282*, 14–22. https://doi.org/10.1016/j.plantsci.2018.06.015

Reynolds, M., Chapman, S., Crespo-Herrera, L., Molero, G., Mondal, S., Pequeño, D., Pinto, F., Pinera Chavez, F., Poland, J., Rivera-Amado, C., Saint, C., & Sukumaran, S. (2020). Breeder friendly phenotyping. *Plant Science, 295*, 110396. https://doi.org/10.1016/j.plantsci.2019.110396

Rizi, M. S., & Mohammadi, M. (2023). Breeding crops for enhanced roots to mitigate against climate change without compromising yield. *Rhizosphere, 26,* 100702. https://doi.org/10.1016/j.rhisph.2023.100702

Robin, A. H. K., & Saha, P. S. (2015). Morphology of lateral roots of twelve rice cultivars of Bangladesh: Dimension increase and diameter reduction in progressive root branching at the vegetative stage. *Plant Root, 9*, 34-42. https://doi.org/10.3117/plantroot.9.34

Rosenqvist, E., Großkinsky, D. K., Ottosen, C. O., & van de Zedde, R. (2019). The phenotyping dilemma—the challenges of a diversified phenotyping community. *Frontiers in Plant Science, 10*(163). https://doi.org/10.3389/fpls.2019.00163

Sharma, N., Singh, B., Krishnan, S. G., Bollinedi, H., Mandal, P. K., Lal, M. K., Jha, P. K., Anand, A., & Vara Prasad, P. V. (2024). Higher grain-filling rate in inferior spikelets of tolerant rice genotype offset grain yield loss under post-anthesis high night temperatures. *Rice Science*, *31*(5), 572–586. https://doi.org/10.1016/J.RSCI.2024.06.003

Shi, L.-D., Ercoli, M. F., Kim, J., Teixeira de Araujo Junior, A., Estera-Molina, K., et al. (2026). Reduced methane emissions in transgenic rice genotypes are associated with altered rhizosphere microbial hydrogen cycling. *Nature Communications*, 17, 2028. https://doi.org/10.1038/s41467-026-68640-9

Shi, W., Raveendran, M., Rahman, H., Selvam, J., Peng, S., Zou, Y., & Jagadish, K. S. V. (2013). Source-sink dynamics and proteomic reprogramming under elevated night temperature and their impact on rice yield and grain quality. *New Phytologist*, *197*(3), 825–837. https://doi.org/10.1111/nph.12088

Soremi, P. A. S., Chirinda, N., & Graterol, E. (2023). Potential of rice (*Oryza sativa* L.) cultivars to mitigate methane emissions from irrigated systems in Latin America and the Caribbean. *All Earth*, *35*(1), 149-157. https://doi.org/10.1080/27669645.2023.2207941

Stella, T., Bregaglio, S., & Confalonieri, R. (2016). A model to simulate the dynamics of carbohydrate remobilization during rice grain filling. *Ecological Modelling*, *320*, 366-371. https://doi.org/10.1016/j.ecolmodel.2015.10.026

Takahashi, H., & Pradal, C. (2021). Root phenotyping: important and minimum information required for root modeling in crop plants. *Breeding Science*, *71*, 109-116. https://doi.org/10.1270/jsbbs.20126

Tanaka, M., Keira, M., Yoon, D. K., Mae, T., Ishida, H., Makino, A., & Ishiyama, K. (2022). Photosynthetic enhancement, lifespan extension, and leaf area enlargement in flag leaves increased the yield of transgenic rice plants overproducing Rubisco under sufficient N fertilization. *Rice, 15*(1):1–15. https://doi.org/10.1186/S12284-022-00557-5

Tang, H., Liu, Y., Li, X., Muhammad, A., & Huang, G. (2019). Carbon sequestration of cropland and paddy soils in China: potential, driving factors, and mechanisms. *Greenhouse Gases: Science and Technology*, *9*(5), 872-885. https://doi.org/10.1002/ghg.1901

Tang, Y., Li, F., Zhou, Z., Huang, H., Guo, T., Wei, X., & Zhuang, J. (2026). DFM-Net: A UAV-based multimodal network for rice SPAD estimation using RGB and thermal infrared images. *Infrared Physics & Technology*, 158, 106796. https://doi.org/10.1016/j.infrared.2026.106796

Tang, Z., Jiang, T., Wang, Y., & Sun, X. (2024). LiDAR: a new player in analyzing plant phenotypes. *Trends in Plant Science*, *29*(12), 1383–1384. https://doi.org/10.1016/j.tplants.2024.10.007

Toyofuku, K., Matsunami, M., & Ogawa, A. (2015). Genotypic variation in osmotic stress tolerance among rice cultivars and its association with L-type lateral root development. *Plant Production Science*, *18*(3), 246-253. https://doi.org/10.1626/pps.18.246

Trumbore, S. (2006). Carbon respired by terrestrial ecosystems – recent progress and challenges. *Global Change Biology*, *12*(2), 141-153. https://doi.org/10.1111/j.1365-2486.2005.01067.x

Tu, D., Jiang, Y., Salah, A., Cai, M., Peng, W., Zhang, L., Li, C., & Cao, C. (2022). Response of source-sink characteristics and rice quality to high natural field temperature during reproductive stage in irrigated rice system. *Frontiers in Plant Science 13*, 911181. https://doi.org/10.3389/fpls.2022.911181

U.S. Department of Agriculture. (2018). *Crop technology readiness level (TRL)*. United States Department of Agriculture National Institute of Food and Agriculture Institute of Food Production and Sustainability. https://www.nifa.usda.gov/sites/default/files/resources/Crop-Research-Technology-Readiness-Level-2018.pdf

Ueda, T., Taniguchi, Y., Adachi, S., Shenton, M., Hori, K., & Tanaka, J. (2025). Gene pyramiding strategies for sink size and source capacity for high-yield japonica rice breeding. *Rice, 18*(6). https://doi.org/10.1186/s12284-025-00756-w

Vaughan, D. A., Lu, B. R., & Tomooka, N. (2008). The evolving story of rice evolution. *Plant Science, 174*, 394-408. https://doi.org/10.1016/j.plantsci.2008.01.016

Vishwakarma, C., Krishna, G. K., Kapoor, R. T., Mathur, K., Dalal, M., Singh, N., Mohapatra, T., & Chinnusamy, V. (2024). Physiological analysis of source–sink relationship in rice genotypes with contrasting grain yields. *Plants, 13*(62). https://doi.org/10.3390/plants13010062

Wang, H., Inukai, Y., & Yamauchi, A. (2006). Root development and nutrient uptake. *Critical Reviews in Plant Sciences*, *25*(3), 279–301. https://doi.org/10.1080/07352680600709917

Watt, M., Fiorani, F., Usadel, B., Rascher, U., Muller, O., & Schurr, U. (2020). Phenotyping: New windows into the plant for breeders. *Annual Reviews of Plant Biology, 71*, 689-712. https://doi.org/10.1146/annurev-arplant-042916-041124

Wen, T., Li, J. H., Wang, Q., Gao, Y., Hao, G., & Song, B. (2023). Thermal imaging: The digital eye facilitates high-throughput phenotyping traits of plant growth and stress responses. *Science of The Total Environment, 899*, 165626. https://doi.org/10.1016/j.scitotenv.2023.165626

Win, E. P., Win, K. K., Bellingrath-Kimura, S. D., & Oo, A. (2020). Greenhouse gas emissions, grain yield and water productivity: a paddy rice field case study based in Myanmar. *Greenhouse Gases: Science and Technology, 10*(5), 884-897. https://doi.org/10.1002/ghg.2011

Wu, Z. H., Yang, C. W., & Yang, M. Y. (2014). Photosynthesis, photosystem II efficiency, amino acid metabolism and ion distribution in rice (*Oryza sativa* L.) in response to alkaline stress. *Photosynthetica, 52*(1), 157-160. https://doi.org/10.1007/s11099-014-0002-4

Xiong, D. (2024). Perspectives of improving rice photosynthesis for higher grain yield. *Crop and Environment, 3*(3), 123-137. https://doi.org/10.1016/j.crope.2024.04.001

Xiong, D., Wang, D., Liu, X., Peng, S., Huang, J., & Li, Y. (2016). Leaf density explains variation in leaf mass per area in rice between cultivars and nitrogen treatments. *Annals of Botany, 117*(6), 963–971. https://doi.org/10.1093/aob/mcw022

Xu, D., Zhu, Y., Chen, Z.-F., Han, C., Hu, L., Qiu, S., et al. (2020). Yield characteristics of japonica/indica hybrids rice in the middle and lower reaches of the Yangtze River in China. *Journal of Integrative Agriculture, 19*(10), 2394–2406. https://doi.org/10.1016/S2095-3119(19)62872-8

Yadav, G. S., Babu, S., Das, A., Bhowmik, S. N., Datta, M., & Singh, R. (2019). Soil carbon dynamics and productivity of rice–rice system under conservation tillage in submerged and unsubmerged ecologies of Eastern Indian Himalaya. *Carbon Management, 10*(1), 51-62. https://doi.org/10.1080/17583004.2018.1545518

Yang, J., & Zhang, J. (2010). Crop management techniques to enhance harvest index in rice. *Journal of Experimental Botany, 61*(12), 3177-3189. https://doi.org/10.1093/jxb/erq112

Yang, J., & Zhang, J. (2023). Simultaneously improving grain yield and water and nutrient use efficiencies by enhancing the harvest index in rice. *Crop and Environment, 2*(3), 157-164. https://doi.org/10.1016/j.crope.2023.07.001

Yang, X., Shi, H., Stovall, A., Guan, K., Miao, G., Zhang, Y., et al. (2018). FluoSpec 2: An automated field spectroscopy system to monitor canopy solar-induced fluorescence. *Sensors, 18*(2063). https://doi.org/10.3390/s18072063

Ye, H., Wang, Z., Zhong, D., Martini, D., Zhang, Q., Jiang, Y., Ding, Y., & Wang, S. (2026). Depicting the response of crop photosynthesis to elevated CO2: The unique role of sun-induced chlorophyll fluorescence. *Agricultural and Forest Meteorology*, 385, 111211. https://doi.org/10.1016/j.agrformet.2026.111211

Ye, M., Zhang, Z., Huang, G., Xiong, Z., Peng, S., & Li, Y. (2020). High leaf mass per area *Oryza*geno types invest more leaf mass to cell wall and show a low mesophyll conductance. *AoB PLANTS, 12*(4), plaa028. https://doi.org/10.1093/aobpla/plaa028

Ye, M., Zhang, Z., Huang, G., & Li, Y. (2022). Leaf photosynthesis and its temperature response are different between growth stages and N supplies in rice plants. *International Journal of*

Molecular Sciences, *23*(7). https://doi.org/10.3390/ijms23073885

Zang, Y., Wu, G., Li, Q., Xu, Y., Xue, M., et al. (2024). Irrigation regimes modulate non-structural carbohydrate remobilization and improve grain filling in rice (*Oryza sativa* L.) by regulating starch metabolism. Journal of Integrative *Agriculture*, *23*(5),1507-1522. https://doi.org/10.1016/j.jia.2023.05.012

Zhang, J., Li, G., Huang, Q., Liu, Z., Ding, C., Tang, S., Chen, L., Wang, S., Ding, Y., & Zhang, W. (2017). Effects of culm carbohydrate partitioning on basal stem strength in a high-yielding rice population. *The Crop Journal 5*(6), 478-487. https://doi.org/10.1016/j.cj.2017.08.008

Zhao, Y., Wu, J., Flo, V., Wang, J., Zhang, Q., & Mencuccini, M. (2026). Thermal regulation shapes the coordination of stomatal conductance, transpiration, and photosynthesis in rice. *Journal of Experimental Botany*, erag484. https://doi.org/10.1093/jxb/erag484

Zheng, Z., Huang, J., Tian, M., Liu, H.-J., Li, X., Sun, Y., et al. (2026). A dual-substrate X-ray CT platform for in situ high-resolution and high-throughput phenotyping of crop root systems. *Plant Physiology*, 201(3), kiag197. https://doi.org/10.1093/plphys/kiag197

Zhu, X. G., Long, S. P., & Ort, D. R. (2010). Improving photosynthetic efficiency for greater yield. *Annual Review of Plant Biology*, *61*, 235-261. https://doi.org/10.1146/annurev-arplant-042809-112206

Zhu, Z., Ge, T., Xiao, M., Yuan, H., Wang, T., Liu, S., Atere, C. T., Wu, J., & Kuzyakov, Y. (2017). Belowground carbon allocation and dynamics under rice cultivation depends on soil organic matter content. *Plant and Soil*, *410*, 247–258. https://doi.org/10.1007/S11104-016-3005-z

Zou, J., Xu, H., Qin, B., Lan, C., Li, J., Zhang, B., et al. (2026). Ratoon season rice reduces methane emissions by limiting acetic acid transport to the rhizosphere and inhibiting methanogens. *Advanced Science*, 13, e07916. https://doi.org/10.1002/advs.202507916